AN5528

Application note

Radio communication range estimation in ISM band

Introduction

This document is an introduction to prediction and practical testing of radio communication range. The communication range of low power radio is influenced by several factors and this document helps users to understand the role of the key contributors, suggesting how to tune and tradeoff between them.

This application note presents some prediction models based on existing literature. Some practical results achieved by ST sub GHz (S2-LP) and 2.4 GHz (BlueNRG family) radio are provided along with the comparison with prediction models. Finally, some common issues about the communication range are presented along with some possible solutions.

1 Radio signal propagation introduction

This section introduces some useful concepts necessary, in a preliminary stage, to estimate a radio communication distance but also to overcome potential critical issues occurring in the phase of the experimental measurement on the field.

An exhaustive discussion would involve a theoretical dissertation, which is beyond the purpose of this document. However, for further details, you can refer to the book referenced in Section 5 Bibliography.

The concepts presented are:

- Free space path loss
- Multipath effect in radio communication
- Two-ray ground propagation model
- Log-distance path loss model
- Antenna parameters
- Noise floor and self-jamming

1.1 Free space propagation model

Free space path loss model (FSPL) is a model used to predict the power loss of an electromagnetic wave, which propagates through free space without close obstacles that could cause reflection or diffraction.

Eq. (1), known as the Friis equation, calculates the power received from a receiver antenna which is separated from a transmitting antenna by a distance d. This equation is accurate in far field condition only, where spherical spreading can be assumed.

$$P_R = P_T \times G_T \times G_R \times \left(\frac{\lambda}{4\pi d}\right)^2 \quad (1)$$

- P_T: conducted power transmitted
- P_R: power received
- d is the distance between transmitter and receiver
- λ is the wavelength
- G_R: gain in receiving antenna
- G_T: gain in transmitting antenna

For the ideal isotropic antenna, free space loss in decibel is:

$$FSLP_{dB} = 10 \times \log_{10}\frac{P_T}{P_R} = 10 \times \log_{10}\left(\frac{(4\pi d)^2}{\lambda^2 \times G_T \times G_R}\right) \quad (2)$$

Eq. (2) can be rewritten as reported below where the distance d between transmitter and receiver is expressed in Km and the frequency in MHz.

$$FSPL'(dB) = 20 \times \log_{10} d + 20 \times \log_{10} f - 10\log_{10}(G_T \times G_R) + 32.44 \quad (3)$$

- d is the distance between transmitter and receiver in Km
- f is the frequency in MHz

A theoretical range estimation can be done matching the link budget and the free space path loss definitions.

$$Link\ budget = 20 \times \log_{10} d + 20 \times \log_{10} f + 32.44 \quad (4)$$

Here is an example which gives an idea of the communication range estimation obtained using the Friis model:

- frequency = 868 MHz
- data rate = 38.4 kbps
- frequency deviation = 20 kHz
- Channel filter = 100 kHz
- P_{TX_MAX} = 16 dBm
- S_{RX} = -110 dBm

$$Link\ budget = 16\ dBm - (-110)dBm = 126\ dB \quad (5)$$

$$FSPL'(dB) = 20 \times \log_{10} d + 20 \times \log_{10} 868MHz + 32.44 \quad (6)$$

$$d = 10^{[Link\ budget\ - 20 \times \log_{10}(f) - 32.44]/20} \quad (7)$$

$$d = 10^{[126\ - 20 \times \log_{10}(868) - 32.44]/20} = 54\ Km \quad (8)$$

1.2 Multi-path propagation

The free space propagation model assumes that between the transmitter and receiver an unobstructed path (line-of-sight path) exists and only one medium for the propagation.

In a real-world environment, a single direct path between the transmitter and receiver is unlikely and the most common case is when obstacles between the transmitter and receiver modify the propagation of the radio signal.

The multi–path propagation describes the mode of propagation of the radio signal when obstacles are present between receiver and transmitter and the RF signal travels over multiple paths.

The multi-path model classifies the incident of waves on the receiver antenna into four types:

- Direct waves: waves which travel on a line-of-sight path.
- Reflected waves: when the direct wave impinges upon objects or a surface that have very large dimensions when compared to one wavelength.
- Diffracted waves: when surfaces are present between transmitter and receiver with sharp corners (edges).
- Scattered waves: when objects are present between transmitter and receiver with dimensions that are much smaller than one wavelength.

When multipath phenomenon occurs, multiple copies of the transmitted signal reach the receiving antenna travelling on different paths and therefore, the received total power is the sum vector of multiple signals with different magnitudes and phase shift.

The waves coming from multipath can be considered as interferences which can give a constructive or destructive contribution to the power seen at the receiver causing variations of the signal strength.

1.3 Ground reflection model

One of the aims of this application note is to provide a mathematical model for the estimation of the communication range. The model is based on the well-known two-ray model where the received power is calculated as the sum of two components: the power coming from the line of sight wave and the power coming from the wave reflected by the ground plane.

For this reason, in this section, a brief description of the ground reflection phenomena is given.

When an electromagnetic wave impacts upon an interface between two mediums with different electrical properties, the incident wave is partially reflected and partially transmitted. The reflection depends on the direction of the polarization of the E-field.

The incident wave with an arbitrary E-field polarization can be decomposed into two polarization components: a component parallel to the plane of incidence and a component normal to plane of incidence where the plane of incidence is defined as the plane containing the incident, the reflected and the transmitted rays.

The Fresnel equations provide the relationship between electric field intensities of the reflected and incident waves.

The derivation of the Fresnel equation is based on Snell’s law and the boundary relations for the electric and magnetic fields at the interface between two media with different electromagnetic properties.

Figure 1. **Reflection model**

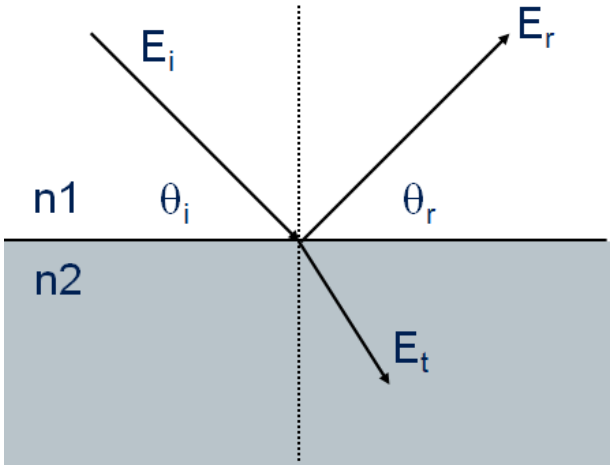

If the incident medium is the air and the reflecting medium has a permeability $\mu_1 = \mu_2$ then we obtain the following Fresnel equations for two cases of vertical and horizontal polarization. If the E-field is parallel to the plane of incidence, we have the following equation:

$$\Gamma_{||} = \frac{E_r}{E_i} = \frac{-\varepsilon_r \sin\theta_i + \sqrt{\varepsilon_r - \cos^2\theta_i}}{\varepsilon_r \sin\theta_i + \sqrt{\varepsilon_r - \cos^2\theta_i}} \quad (9)$$

If the E-field is orthogonal to the plane of incidence we have:

$$\Gamma_{\perp} = \frac{E_r}{E_i} = \frac{\sin\theta_i - \sqrt{\varepsilon_r - \cos^2\theta_i}}{\sin\theta_i + \sqrt{\varepsilon_r - \cos^2\theta_i}} \quad (10)$$

If the direction of the antenna is orthogonal to the ground, the E-field is parallel to the plane of incidence and the reflection coefficient to use is Γ||.

If the direction of the antenna is parallel to the ground, the E-field is orthogonal to the plane of incidence and the reflection coefficient to use is Γ^.

The reflection coefficient, reported above, has been used in our mathematical model to calculate the effect of the reflection wave on the total received power.

Figure 2. **Reflection coefficient vs. incident angle for sand (ε_r=2.5)**

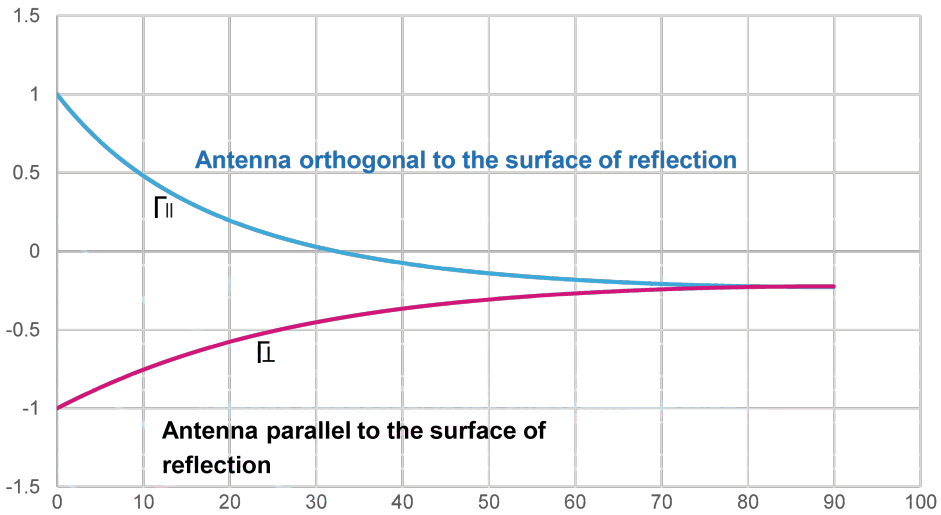

Figure 3. **Module of reflection coefficient vs. incident angle for sand (ε_r=2.5)**

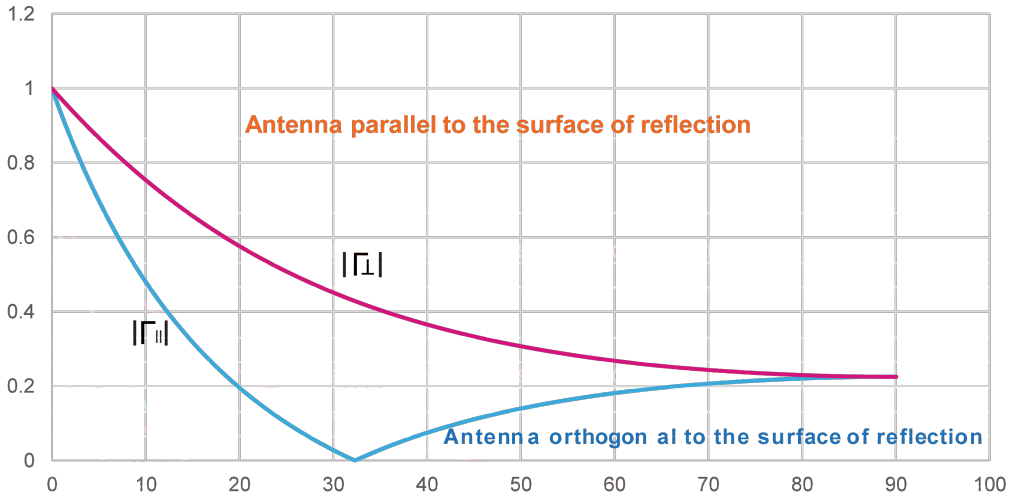

Figure 4. **Reflection coefficient vs. incident angle for soil (ε_r=18)**

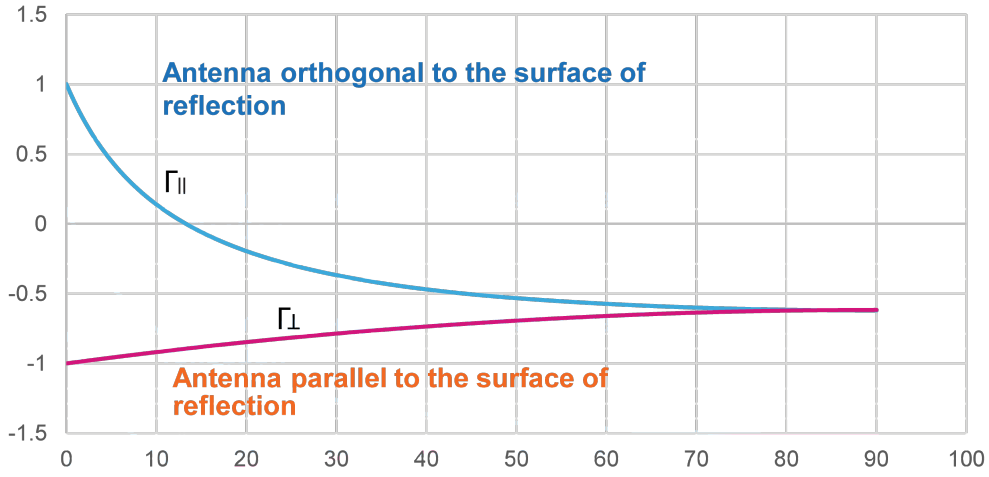

Figure 5. **Module of reflection coefficient vs. incident angle for soil (ε_r=18)**

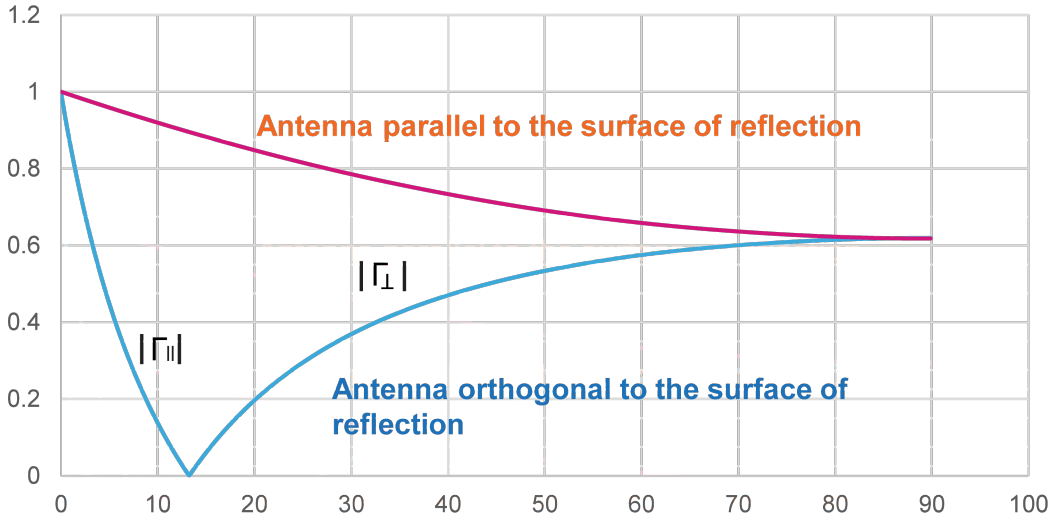

1.4 Two-ray ground propagation model

The two-ray propagation model is the simplest model which considers the effect of the multipath phenomenon.

This model assumes the interaction between two electric fields that reach the receiver. The former is related to the line of sight propagation path and the latter is related to the wave reflected in by a flat ground surface.

Reflected signal may arrive out of phase with the direct wave and then reduce the power of the received signal or on the other hand it may enhance the power of the received signal if it arrives in phase.

Figure 6. **2-ray ground reflection diagram**

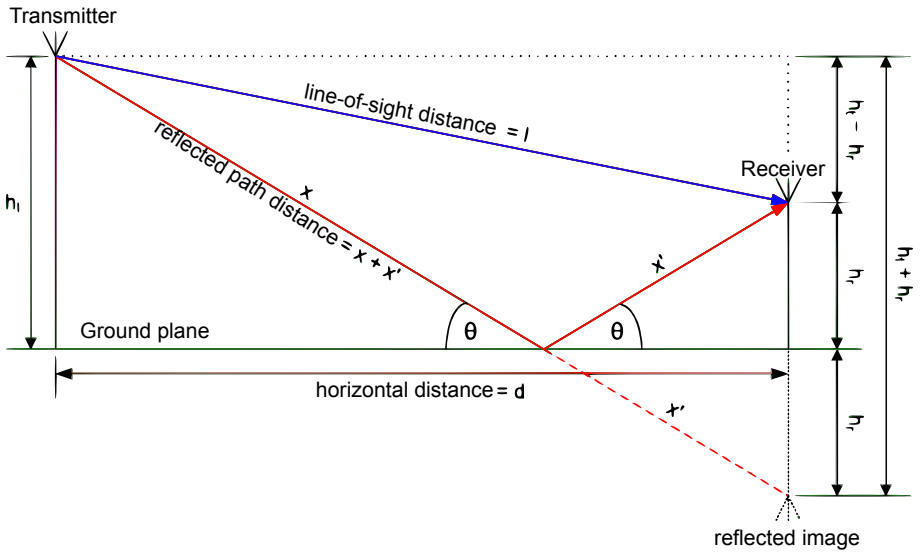

The first step calculates the phase shift between the direct and reflected waves. This phase shift is due to the different path length of direct and reflected wave. We denote h_t the height of the antenna transmitter, with h_r the height of the receiver antenna and with d the distance over a flat earth between the transmitter and the receiver.

The line of sight path distance is given by:

$$d_{LOS} = \sqrt{(h_t - h_r)^2 + d^2} \quad (11)$$

The length of the ground reflected path is given by:

$$d_{reflected} = \sqrt{(h_t + h_r)^2 + d^2} \tag{12}$$

Phase difference between the E-field vectors of the direct wave E_{LOS} and the reflected wave E_{REFL} is given by:

$$\varphi_\Delta = \frac{2\pi}{\lambda}\left(d_{reflected} - d_{LOS}\right) = \frac{2\pi f_c}{\lambda f_c}\left(d_{reflected} - d_{LOS}\right) = \frac{\omega_c}{c}\left(d_{reflected} - d_{LOS}\right) \tag{13}$$

If E_0 is the reference value for the electric field intensity, measured at a reference distance d_0 (1 meter) from the transmitter, then the equation that describes the free space propagation of the E-field is given by:

$$E(d,t) = \frac{E_0 d_0}{d}\cos\left[\omega_c\left(t - \frac{d}{c}\right)\right] \tag{14}$$

The total electric field is the sum of the E-field due to the line of sight component and the E-field due to the ground reflected wave:

$$E_{TOT}(d_{LOS},t) = \sqrt{E_{LOS}(d_{LOS},t)^2 + E_{REFL}(d_{REFL},t)^2 + 2\,E_{LOS}(d_{LOS},t)E_{REFL}(d_{LOS},t)\cos\varphi_\Delta} \tag{15}$$

where

$$E_{LOS}(d_{LOS},t) = \frac{E_0 d_0}{d_{LOS}}\cos\left[\omega_c\left(t - \frac{d_{LOS}}{c}\right)\right] \tag{16}$$

$$E_{REFL}(d_{REFL},t) = \Gamma\frac{E_0 d_0}{d_{REFL}}\cos\left[\omega_c\left(t - \frac{d_{REFL}}{c}\right)\right] \tag{17}$$

In Eq. (17) the E-field component due to the reflected wave is multiplied by the ground reflection coefficient Γ. To compute this coefficient we need to derivate the angle of incidence as:

$$\theta_i = \tan^{-1}\left(\frac{h_t + h_r}{d}\right) \tag{18}$$

$$E_{TOT}(d_{LOS},t) = \frac{E_0 d_0}{d_{LOS}}\cos\left[\omega_c\left(t - \frac{d_{LOS}}{c}\right)\right] + \Gamma\frac{E_0 d_0}{d_{REF}}\cos\left[\omega_c\left(t - \frac{d_{REF}}{c}\right)\right] \tag{19}$$

Now we evaluate the intensity of the E-field of the direct wave in the instant in which the direct wave reaches the receiver replacing the variable t with:

$$t = \frac{d_{LOS}}{c} \tag{20}$$

$$E_{LOS}\left(d_{LOS}, t = \frac{d_{LOS}}{c}\right) = \frac{E_0 d_0}{d_{LOS}}\cos\left[\omega_c\left(\frac{d_{LOS}}{c} - \frac{d_{LOS}}{c}\right)\right] = \frac{E_0 d_0}{d_{LOS}} \tag{21}$$

To calculate the E-field intensity of the reflected wave we consider the effect of the length of the reflected path d_{REF} and the ground reflection coefficient:

$$E_{REFL}\left(d_{REF}, t = \frac{d_{LOS}}{c}\right) = \Gamma\frac{E_0 d_0}{d_{REF}} \tag{22}$$

The E_{REFL} E-field component will arrive at the receiver with a phase difference given by Eq. (13) and the intensity of the total E-field is calculated by the vectoral sum between the direct and ground reflected rays:

$$E_{TOT}\left(d_{LOS}, t = \frac{d_{LOS}}{c}\right) = \sqrt{\left(\frac{E_0 d_0}{d_{LOS}}\right)^2 + \left(\Gamma\frac{E_0 d_0}{d_{REF}}\right)^2 + 2\,\Gamma\frac{E_0 d_0}{d_{LOS}}\frac{E_0 d_0}{d_{REF}}\cos\varphi_\Delta} \tag{23}$$

If we consider the vertical polarization, it means the E-field has an orthogonal component with respect to the reflecting surface, then the reflecting coefficient to use is Γ|| (Eq. (9)).

If we consider the horizontal polarization, it means the E-field is parallel to the reflecting surface, then the reflecting coefficient to use is Γ⊥(Eq. (10)).

Assuming perfect horizontal E-field polarization and ground reflection then Γ⊥ = -1 and Et = 0.

If the E-field is assumed to be in the plane of incidence (i.e. vertical polarization) then Γ|| = 1.

The receiver power is a square function of the total electric field.

$$P_r(d) = \frac{P_t G_t G_r \lambda^2}{(4\pi)^2}\left[\left(\frac{1}{d_{LOS}}\right)^2 + \left(\frac{\Gamma}{d_{REF}}\right)^2 + \frac{2\Gamma\cos\varphi_\Delta}{d_{REF}\,d_{LOS}}\right] \tag{24}$$

Rappaport [1] in Section 5 Bibliography assumes that for very large distance the difference between the direct and reflected paths is very small and the amplitudes of the E-fields are identical and differ only in phase.

So, with this assumption we have:

$$\frac{E_0 d_0}{d} \approx \frac{E_0 d_0}{d_{LOS}} \cos\varphi_\Delta \approx \frac{E_0 d_0}{d_{REF}} \quad (25)$$

Another assumption in Rappaport [1] Section 5 Bibliography is the perfect polarization and reflection that means |Γ| = 1. Thanks to these exemplifications, Rappaport [1] (Section 5 Bibliography) provides the following two-ray ground path loss equation.

$$Pr_{dB} = P_t \times G_T \times G_R 10 \times \frac{h_T^2 h_t^2}{d^4} \quad (26)$$

Section 2.1 Measurement #1: logarithmic trend of RSSI, Section 2.2 Measurement #2: comparison between 433 MHz and 868 MHz band, Section 2.3 Measurement #3: Test in 433 MHz band and Section 2.4 Measurement #4: Test in 2.4 GHz band (Bluetooth Low Energy) present some experimental results for various radio configuration and band that demonstrate the accuracy of the model presented so far.

1.5 Log-distance path loss model

An empirical model to predict radio communication distances is based on the observation that the relationship between distance and path loss is logarithmic. The model offers an empirical way on how to calculate the path loss exponent in a target environment.

The far-field average power, measured over distances of many wavelengths, decreases inversely with the distance:

$$\overline{PL}(dB) = \overline{PL}(d_0) + 10n\log\left(\frac{d}{d_0}\right) \quad (27)$$

$$\overline{PL}(d_0) = 20\log\left(\frac{4\pi d_0}{\lambda}\right) \quad (28)$$

- d_0 is a reference distance from antenna, also called ***close-in reference distance***, (usually 10 to 100 m outdoor) which is obtained by using Friis path loss equation or by field measurements at d_0
- n is the path loss exponent that depends on the type of environment, as given in the table below

The path loss exponent indicates the rate at which the path loss increases with distance and can be computed by the formula:

$$n = \frac{\overline{PL}(d) - \overline{PL}(d_0)}{10\log\left(\frac{d}{d_0}\right)} \quad (29)$$

Table 1. Path loss exponent for different environments lists typical path loss exponents obtained in various environments.

Table 1. Path loss exponent for different environments

Environment	Path loss exponent (n)
Free space	2
Urban area cellular radio	2.7 to 3.5
Shadowed urban cellular radio	3 to 5
Inside a building - line-of-sight	1.6 to 1.8
Obstructed in building	4 to 6
Obstructed in factory	2 to 3

1.6 Antenna parameters

The decision of the antenna plays a fundamental role for getting good performance in terms of radio propagation.

An antenna is a transducer that converts the power at its input port-to-power radiated in the space and vice versa. It can be demonstrated that the antenna performance is identical for both transmitting and receiving functions.

An antenna radiation pattern is a 3D representation of the power radiated in the space. In the figure below, an example of radiation pattern is shown.

Figure 7. **Antenna radiation pattern example**

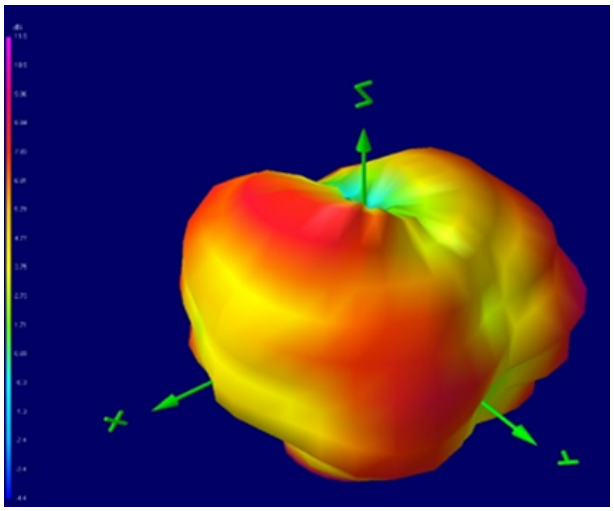

It is important to know that the radiation pattern is not only a function of the antenna itself, but it depends also on the overall system including PCB layout, ground plane size, space and mechanical surroundings.

The antenna key parameters are:

- Total radiated power, TRP (dBm): calculated by integrating the radiated power measured in all directions
- Peak EIRP (dBm): the maximum value of measured radiated power
- Directivity (dBi): the difference from the peak EIRP and TRP
- Efficiency (%): the difference between the TRP and the input power delivered to the DUT
- Gain (dBi): the sum of efficiency and directivity
- Effective isotropic radiated power EIRP (dBm): the total power that would have to be radiated by a lossless isotropic antenna to give the same signal strength as the current source in the direction of the strongest antenna beam

$$EIRP = \mathrm{P}_{TX}(dBm) + G_T(dBi) \quad (30)$$

- Effective radiated power, ERP (dBm): the total power that would have to be radiated by a half-wave dipole antenna to give the same signal strength in watts per square meter as the actual source at a distant receiver located in the direction of the strongest antenna beam (main lobe)

Relationship between the EIRP and ERP:

$$EIRP = \mathrm{P}_{TX}(dBm) + G_T(dBi) \quad (31)$$

$$\boldsymbol{ERP} = \mathrm{P}_{TX} + G_T(dBi) - 2.15\ dB \quad (32)$$

- Effective aperture: the effective area Aw of an antenna is a parameter especially defined for receiving antennas. It is a measurement for the maximum received power Pr that an antenna can pick up from a plane wave with a power density S:

$$\mathrm{Pr\,max} = S \times Ae \quad (33)$$

Although the effective area of an antenna can be well-conceived as a real area perpendicular to the direction of propagation of the incident wave, it is not necessarily the same as the geometrical area Ag of the antenna.

The relationship between the effective and the geometrical areas is described by the aperture efficiency q:

$$q = AeAg \quad (34)$$

The effective area of an antenna can be converted to the gain and vice versa by the formula below:

$$Ae = \left(G_R\lambda^2\right)/(4\pi) \quad (35)$$

Figure 8. **Power flux density at a distance d from a point source**

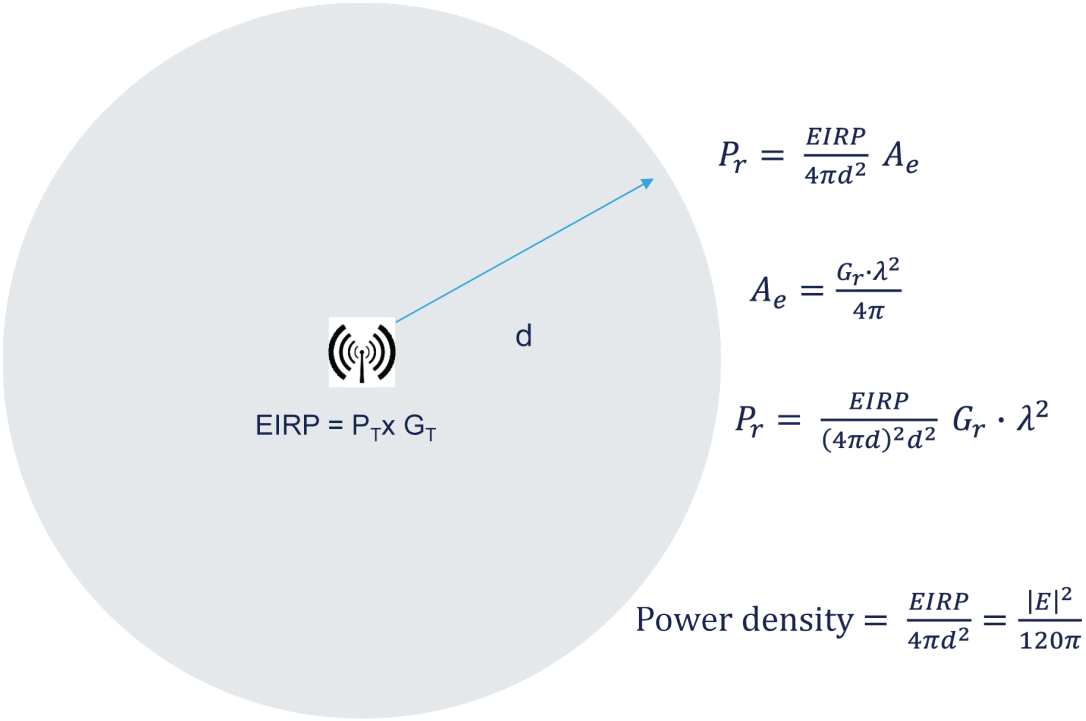

1.7 Noise floor

Another key parameter that plays a role in the radio communication distance is the noise floor observed in the environment where the radio communication is performed. In absence of any environmental noise floor and for a select bandwidth, the noise floor of radio is calculated as the sum of the thermal noise.

See the Eq. (36)

$$TN_{dBm} = 10 \times log_{10}\left[K \times T \times BW \times 10^3\right] \quad (36)$$

where:

- *K* is the Boltzmann constant 1.38064852 × 10^{-23} m^2 kg s^{-2} K^{-1}
- *T* is the temperature expressed in kelvin
- *BW* is the receiver bandwidth in Hz

For instance, at 25 °C and with a channel filter of 100 kHz the thermal noise is:

$$10x\log 10\left[1.38x10^{-23}x298.15x100.000x1000\right] = -123.8dBm \quad (37)$$

The noise floor level can be obtained adding the noise figure of the transceiver and the thermal noise. The noise figure (NF) is a measure of the amount of noise added by the receiver itself by its internal circuitry.

$$Noise\ floor = TN_{dBm} + NF \quad (38)$$

For example, considering a radio receiver with noise figure equal to 8 dB, the overall noise floor is -115.8 dBm.

The value calculated with Eq. (36) represents a low-level watermark that can never be crossed.

In real cases, the noise floor grows due to other contributors such as:

- Environmental noise
- PCB generated noise

Environmental noise and PCB generated noise also degrade the performance of the receiver by increasing the noise level. This kind of noise is dependent on the environment, the frequency band and the PCB and it is more subtle to characterize. PCB generated noise, also called self-jamming, is a parameter that needs to be investigated in order to achieve the optimal radio receiver performance.

1.8 Sensitivity

The sensitivity is defined as the minimum power level of the wanted signal required to achieve a fixed minimum signal quality measured by bit error rate or packet error rate.

In digital modulation systems the sensitivity performance is measured using two different benchmarks: bit error rate (BER) or packet error rate (PER).

Packet error rate (PER): defined as the ratio between the number of wrong packets received and the total number of transmitted packets. A packet is said to be wrong even if there is only one erroneous bit.

The relationship between the BER and PER is valid for an ideal communication system that transmits data over the binary symmetric channel with uncorrelated noise. This relationship is not valid for correlated noise channels and is dependent on the specific receiver implementation. The length of the packet in bits is n and the bit error probability for the channel is BER. Any packet that has one bit or more in error is discarded and the probability of getting a packet in error is given by:

$$PER = 1 - (1 - BER)^n \tag{39}$$

Usually, in radio communication, PER is more useful at applicative level. PER measurements verify all the internal circuit functions, such as: bit timing acquisition, AFC error correction, Preamble detection, Sync Word detection, CRC checksum calculation, and interrupt handling.

The sensitivity values reported in the datasheet are measured in conducted mode and this value can be used to determineate the minimum signal to noise ratio needed to reach the specified error performance.

A theoretical estimation of sensitivity of a receiver can be calculated knowing the following performance parameters: the thermal noise, the noise figure (NF) and the carrier to noise ratio (C/N) required to achieve the desired quality signal.

$$Sensitivity = TN_{dBm} + NF + \frac{C}{N} \tag{40}$$

The difference between sensitivity and noise floor measured gives the minimum signal noise ratio to achieve the fixed bit error rate performance.

The carrier to noise ratio necessary for a receiver to achieve a specified level of reliability in terms of BER is a function of the ratio E_b/N_0, where E_b is the energy per bit and N_0 is the spectral noise density (N_0 = kT) in the baseband signal.

The relationship between BER and E_b/N_0 depends on the digital modulation scheme selected; we report the equation which determinates the necessary E_b/N_0 related to desired bit error rate. For instance, for FSK and ASK:

$$For\ FSK: BER = \frac{1}{2} erfc\sqrt{\frac{1}{2}\frac{E_b}{N_0}} \tag{41}$$

$$For\ ASK: BER = \frac{1}{2} erfc\sqrt{\frac{1}{4}\frac{E_b}{N_0}} \tag{42}$$

Where *erfc* is the complementary error function defined as:

$$erfc(x) = \frac{2}{\sqrt{\pi}}\int_x^\infty e^{-t^2} dt \tag{43}$$

The required received power C/N can be obtained by the following relationship:

$$CNR_{dB} = 10 \times log_{10}\left(\frac{E_b}{N_o}\right) + 10 \times log_{10}\left(\frac{DR}{B}\right) \tag{44}$$

Where:

- E_b is the energy per bit
- N_0 is the noise spectral density (noise power in a 1 Hz bandwidth, measured in watts per hertz or joules)
- *DR* is the data rate in bits per second
- BW is the receiver equivalent noise bandwidth

Figure 6 shows the bit error rate curves for FSK and ASK binary modulation schemes. The x-axis has E_b/N_0 in dB and the y-axis has the probability of error on a logarithmic scale.

Figure 9. **BER vs. Eb/N0 for FSK and ASK modulation**

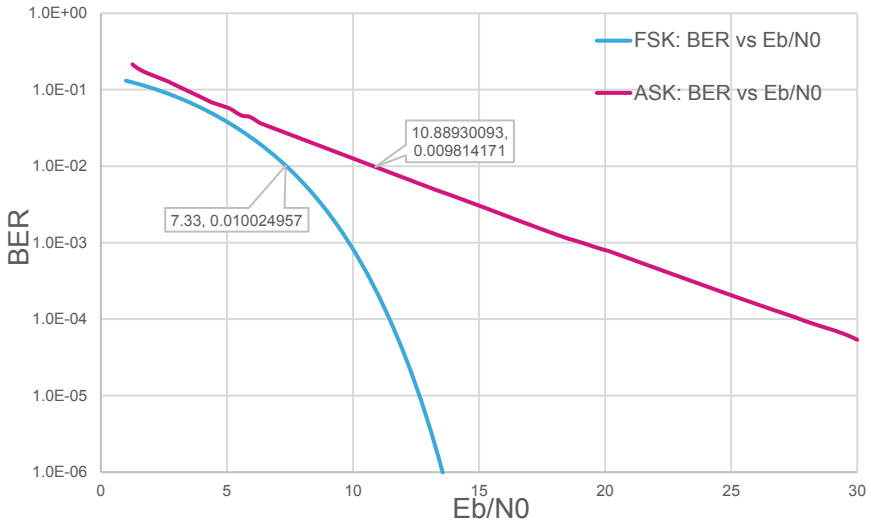

For FSK modulation, the ratio between the separation of the frequency and the data rate is called modulation index.

$$n = \frac{2 \times frequency\ deviation}{data\ rate} \tag{45}$$

Using the Carson rule, we can estimate the bandwidth of the modulated signal:

$$BW = 2 \times fdeviation + Datarate \tag{46}$$

If the modulation index is 1, the bandwidth is twice the data rate. In this case, the modulation is called orthogonal FSK.

Another important parameter is the ratio between the data rate and transmission bandwidth; this parameter is called bandwidth efficiency. For an OFSK modulation with modulation index 1 the bandwidth efficiency is 0.5.

$$Sensitivity = Floor\_noise + \ CNR_{dB} = TN_{dBm} + NF + 10log_{10}\left(\frac{E_b}{N_o}\right) + 10 \times log_{10}\left(\frac{DR}{B}\right) \tag{47}$$

Here the carrier to noise values for FSK and ASK modulation for a target BER fixed to 1%:

$$OFSK\colon CNR_{dB} = 7.33 + 10log_{10}\left(\frac{DR}{BW}\right) \tag{48}$$

$$ASK\colon CNR_{dB} = 10.89 + 10log_{10}\left(\frac{DR}{BW}\right) \tag{49}$$

So the sensitivity is:

$$FSK\colon Sensitivity = Floor\_noise + \ CNR_{dB} = TN_{dBm} + NF + 7.33 + 10log_{10}\left(\frac{DR}{BW}\right) \tag{50}$$

$$ASK\colon Sensitivity = Floor\_noise + \ CNR_{dB} = TN_{dBm} + NF + 10.89 + 10log_{10}\left(\frac{DR}{BW}\right) \tag{51}$$

For a channel bandwidth of 100 kHz, at 25 °C and with a NF equal to 8

$$Sensitivity = \ -123.8\ \text{dBm} + 8 + 7.33 + 10log_{10}\left(\frac{DR}{BW}\right) = \ -108.47 + \ 10log_{10}\left(\frac{DR}{BW}\right) \tag{52}$$

1.9 Summary

In this section a synthetic view of all parameters discussed so far is given.

In the table below, the key parameters influencing the radio communication range are shown: a ↑ arrow means the higher the better range, a ↓ arrow means the lower the better range.

As discussed in the previous sections, some parameters are interdependent, i.e. you can lower receiver channel filter only by decreasing the datarate.

Table 2. Radio communication range key parameters

Key parameters	Increase range
Transmitter power	↑
Datarate	↓
Receiver channel filter	↓
Antenna gain	↑
Noise floor	↓
Height from ground	↑
Frequency	↓
Channel coding	↑
SNR	↓
Sensitivity	↓

In the figure below, a graphical representation of the key parameters for a radio communication range estimation is displayed.

The graph plots the receiver signal strength in dBm at various distances from the transmitter. A few observations:

- The trend is logarithmic
- The two-ray model gives a far lower range estimation than Friis
- The curves are annotated with the key parameters, ie which curve is affected by them

Figure 10. Radio communication range key parameters

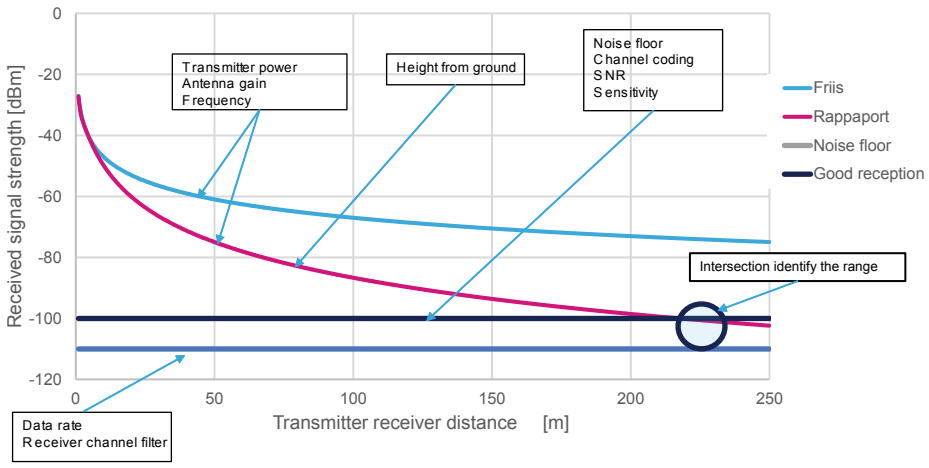

In Figure 10. Radio communication range key parameters there are several curves representing different system measurements versus distance.

These curves are intended to be a qualitative graphical representation to understand the contribution of each parameter listed in Table 2. Radio communication range key parameters.

We have the following curves:

- "Friis" curve represents the RSSI detected at a certain distance from the transmitter, as explained in Eq. (1). We consider this curve more as an upper bound on achievable communication range since it does not take into account reflections and other attenuations.
- "Rappaport" curve represents the RSSI detected at a certain distance from the transmitter as explained in Section 1.4 Two-ray ground propagation model. We consider this as a good approximation for line of sight scenarios.

- "Noise floor" curve represents the noise floor measured in the location where measurements are taken (see Section 1.7 Noise floor).
- "Good reception" curve represents the offset versus noise floor to obtain good reception (see Section 1.8 Sensitivity)

We consider the x-axis value of the cross point between "Rappaport" curve and "Good reception" curve as the estimated communication range.

The annotations on each curve highlight the set of parameters (see Table 2. Radio communication range key parameters), which have an impact on the curve itself and so they give a graphical representation on how parameters influence the radio communication range. For example, if we increase the transmission power, the "Rappaport" curve and “Friis” curve is shifted up and so the cross point between the "Rappaport" curve and "Good reception" curve is moved further away meaning that the range increases. This is a graphical representation of the intuitive concept that increasing transmit power increases the communication range and vice versa.

2 Experimental results

In this section, we present some experimental measurements performed by various ST radios, both sub-1GHz and 2.4 GHz. The aim of the experimental results are to show the key parameters of ST radio and to apply the path loss models for radio communication described in Section 3 Debugging procedure to establish the accuracy of these models on the prediction of the communication range.

Here the list of the input parameters needed for the path loss modelling.

Table 3. Radio communication range model parameters

	Symbol	Description	Unit
TX power	Pout	power delivered to the antenna and measured in conducted mode	dBm
Frequency	f	Center frequency	MHz
TX antenna gain	Gt	Transmitter antenna gain	dBi
RX antenna gain	Gr	Receiver antenna gain	dBi
Noise floor	nf	Environmental noise floor	dBm
TX height	ht	Height from the ground of the transmitter	m
RX height	hr	Height from the ground of the receiver	m
Reflection surface	εr	Reflection surface coefficient: here must be specified the value of the relative permittivity of the reflection surface. Some typical values are: ground (εr = 18), water (εr = 88) and sand (εr = 2.5)	

In order to validate the presented model, we conducted some experiments in different outdoor areas trying to reproduce the line of sight condition.

The RX node is placed at a fixed position and connected to a PC. The RX node simply dumps all the received packets along with a time stamp in a file. Alternatively, the RX node can simply dump the RSSI value.

The TX node is supplied with battery and continuously transmits packets at a fixed rate. The TX node is configured to transmit either a continuous unmodulated tone or modulated packets at a fixed rate. The TX node is moved to a different position for a certain amount of time sufficient to collect a valuable number of data samples. Position data are recorded as GPS coordinates and associated timestamp.

In the GPS plot showing the experiment locations, the RX node is marked with a red spot and the various positions of the TX node are marked in black.

2.1 Measurement #1: logarithmic trend of RSSI

The following experiments have been carried out to demonstrate that the degradation of power versus distance follows a logarithmic trend. In addition to this, a comparison with two-ray model predicted result is shown.

2.1.1 Measurement #1 parameters

Table 4. Measurement #1 test conditions

Name	Value
Sample time	12 seconds
Frequency	433000000 Hz
Datarate	N/A
Modulation	NA
Frequency deviation	NA
RX bandwidth	100000 Hz
TX power	14.31 dBm
TX antenna gain	-2.31 dB
RX antenna gain	-2.31 dB
Antenna orientation	Vertical
TX antenna height	1
RX antenna height	1
εr	18
Board name	STEVAL-FKI433V2
Author	Michele Sardo (STMicroelectronics)
Date	26 December 2018
Location	Floridia (Siracusa), Italy

Figure 11. Measurement #1 location

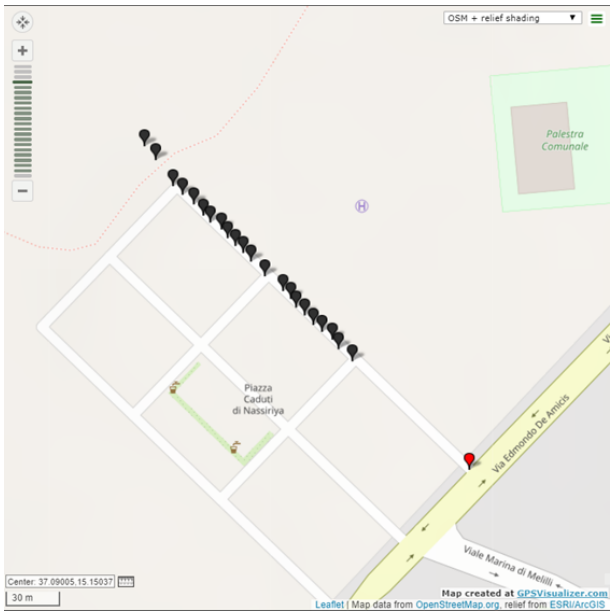

2.1.2 Measurement #1 results

Table 5. Input data used in the mathematical model

	Symbol	Value	Unit
TX power	Pout	14.31	dBm
Frequency	f	433	MHz
TX antenna gain	G_t	-2.31	dB
RX antenna gain	G_r	-2.31	dB
TX height	h_t	1	m
RX height	h_r	1	m
Reflection surface	ε_r	18	

Figure 12. RSSI vs. distance at 433 MHz

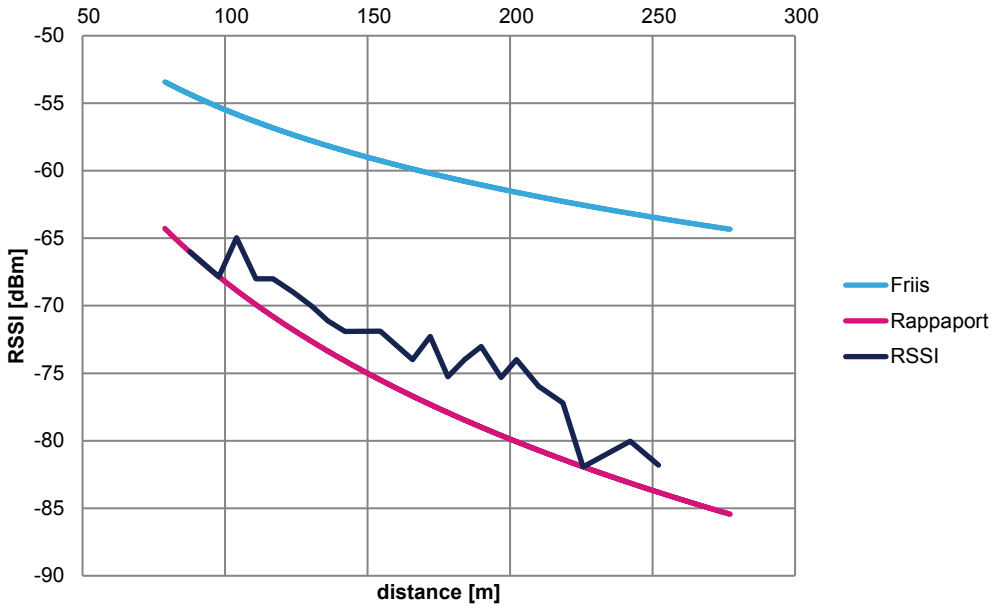

The outcome of this experiment confirms the expectations, that are:

- Logarithmic trend for RSSI vs. distance

The Rappaport two-ray model is a far better estimation compared to Friis.

2.2 Measurement #2: comparison between 433 MHz and 868 MHz band

The aim of this experiment was to assess reliability of the two-ray model and to compare range between 433 MHz and 868 MHz.

2.2.1 Measurements #2 parameters

Table 6. Measurement #2 test conditions

Name	433 MHz	868 MHz	Units
Sample time	12		seconds
Frequency	433	868	MHz
Datarate	1200		bps
Modulation	2-FSK		
Frequency deviation	2400		Hz
RX bandwidth	10000		Hz
TX power	14.31	15.83	dBm
TX antenna gain	-2.31	1.57	dBi
RX antenna gain	-2.31	1.57	dBi
TX antenna height	1		m
RX antenna height	1		m
εr	2.5 (sand)		
Board name	STEVAL-FKI433V2	STEVAL-FKI868V2	
Author	Placido De Vita, Saverio Grutta, Michele Sardo (STMicroelectronics)		
Date	7 February 2019		
Location	Plaia Beach, Catania, Italy		

Figure 13. Measurement #2 location (868 MHz)

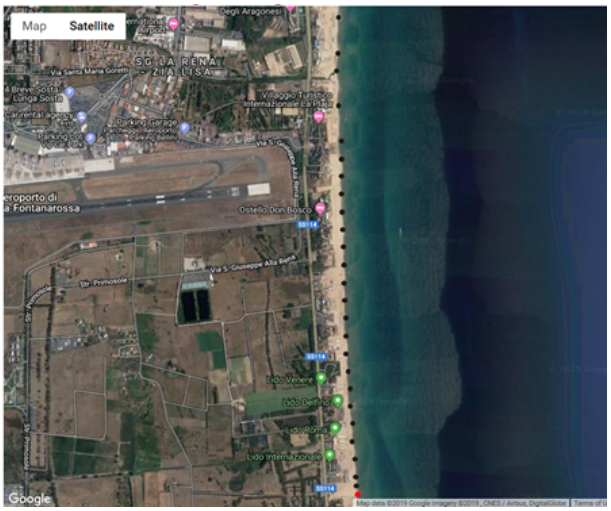

Figure 14. **Measurement #2 location (433 MHz)**

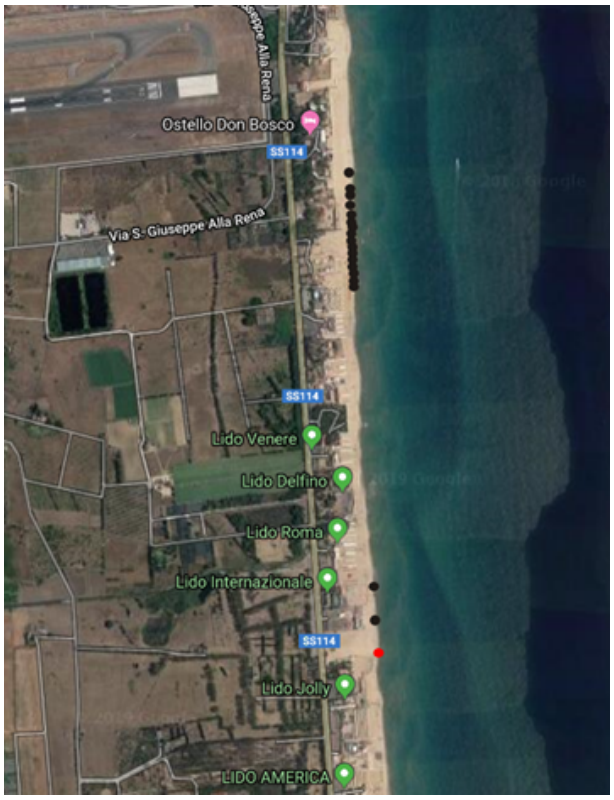

2.2.2 Measurement #2 results

Table 7. **Noise floor comparison 433 MHz vs. 868 MHz**

Noise floor result				
Frequency band		433 MHz	868 MHz	
Noise floor	nf	-116.48	-125.34	dBm

In Figure 15. RSSI vs. distance (868 MHz), we overlay in the same graph the average values of the receiver signal strength obtained in our experiment and two different path loss models: the free-space model given in Equation 2 and the two-ray ground model presented in Section 3.4. In this experiment we reached 2.7 km with packet error rate equal to zero and this is coherent if we consider that the signal-to-noise ratio in the last acquisition point was more than 15 dB.

Figure 15. **RSSI vs. distance (868 MHz)**

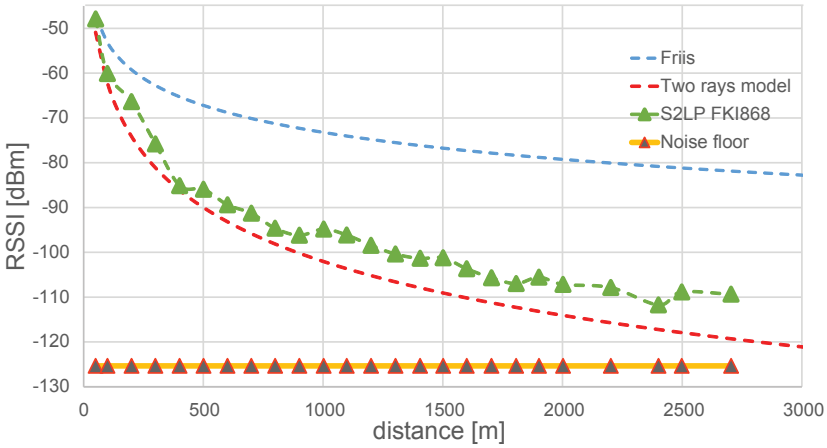

In this test at 433 MHz, we recorded the data until we reached a 100% PER, that is no packet was received. The model crosses the floor noise incremented by 10 dB at about 0.8 km, in the current test the receiver starts to lose packets at around 1.1 km (see Figure 17. Packet error rate vs. distance (433 MHz)).

Some observations worth highlighting:

- RSSI degradation follow logarithmic trend
- The test confirms that the receiver starts to lose packets when the received signal strength is around 10 dB higher than noise environmental floor noise measured using our evalaution board
- The prediction communication range (0.8 km) using the two ray model is a little bit pessimistic on the actual range (1.1 km). This is probably due to the fact that the reflecting surface (sand in our case) is not perfectly flat

Figure 16. **RSSI vs. distance (433 MHz)**

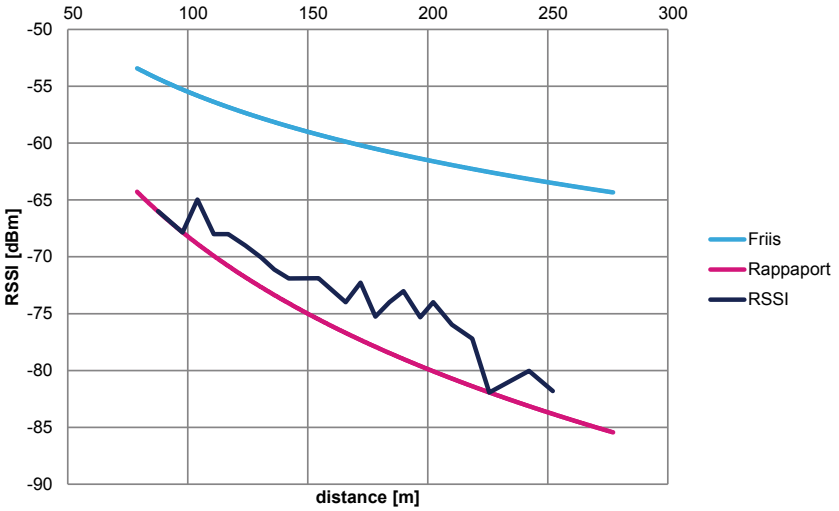

Figure 17. **Packet error rate vs. distance (433 MHz)**

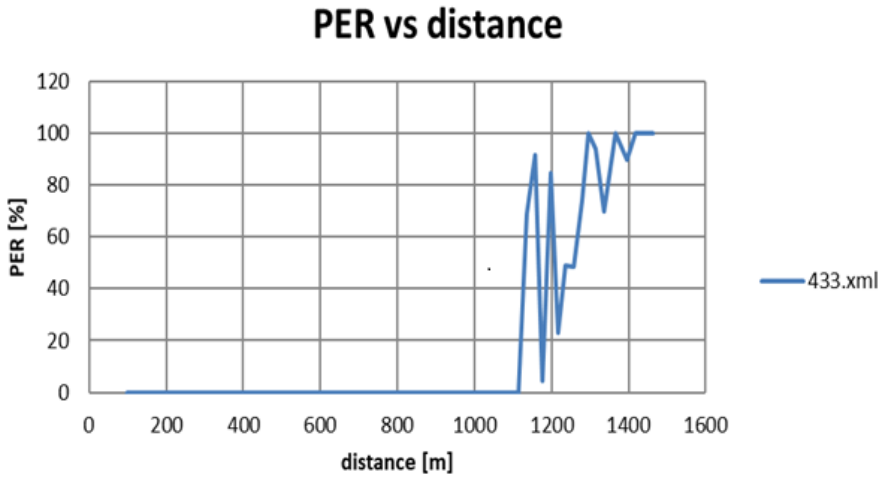

2.2.3 Measurement #2 analysis

This test shows that not only the frequency plays a key role in radio communication range. In fact, the common expectation is that 433 MHz shows a better communication range due to Friis (see Eq. (3)) having an advantage of about 6 dB over 868 MHz, but when we also take into account antenna gain, output power and noise floor, the situation changes in favor of 868 MHz.

Table 8. **Comparison between 433 MHz and 868 MHz**

	STEVAL-FKI433V2	STEVAL-FKI868V2	Unit	Gap	Unit
Pout	14.31	15.83	dBm	1.52	dB
G_t	-2.31	1.57	dBi	3.88	dB
G_r	-2.31	1.57	dBi	3.88	dB
Noise floor	-116.48	-125.34	dBm	8.86	dB
Frequency factor	172.75	178.77	dB	-6.02	dB
Total				**12.12**	dB

2.3 Measurement #3: Test in 433 MHz band

2.3.1 Measurements #3 parameters

Table 9. **Measurements #3: test conditions**

Name	433 MHz	Units
Sample time	12	seconds
Frequency	433	MHz
Data rate	1200	bps
Modulation	2-FSK	
Frequency deviation	2400	Hz
RX bandwidth	10000	Hz
TX power	14.31	dBm

Name	433 MHz	Units
TX antenna gain	-2.31 dB	dBi
RX antenna gain	-2.31 dB	dBi
TX antenna height	1.5	m
RX antenna height	1.5	m
εr	2.5 (sand)	
Board name	STEVAL-FKI433V2	
Author	Helon Chen (STMicroelectronics)	
Date	18 March 2019	
Location	Jiaochangwei beach, Shenzhen, Guangdong province, China	

Figure 18. Measurement #3 location

2.3.2 Measurements #3 results

Figure 19. Measurement #3 RSSI vs. distance

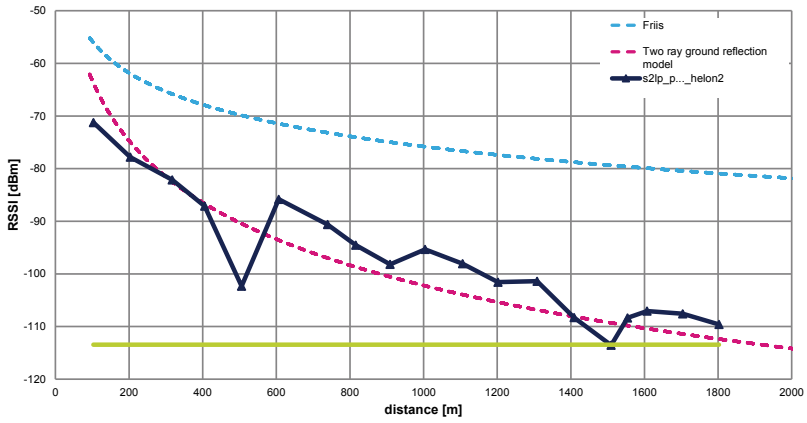

Figure 20. Measurement #3: packet error rate vs. distance

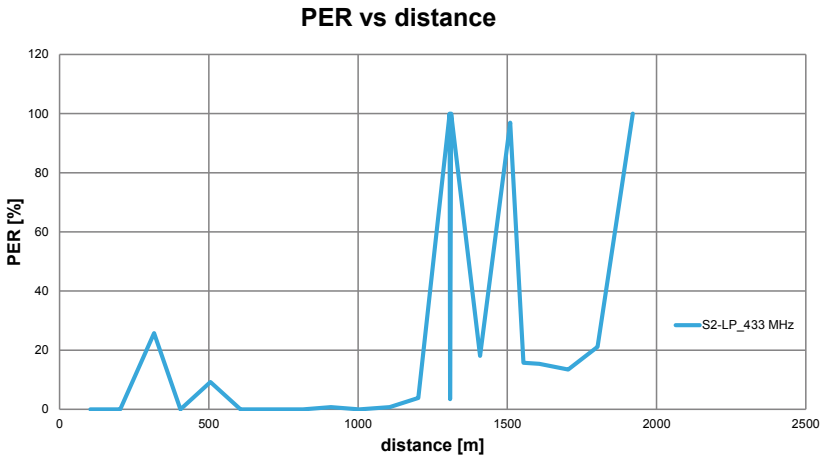

The reported noise floor was -113.44 dBm.

This test confirms that the model represents a good approximation for the current data. Some deviation recorded at about 500 m could be related to people/vehicles altering momentarily the line of sight path. In addition to this, even though the recorded noise floor was higher than previous experiments in different locations (see Table 7. Noise floor comparison 433 MHz vs. 868 MHz), the communication range at PER close to 0% was a little bit higher (1.2 km vs. 1.1 km); this could be justified by the fact that the antenna height was 1.5 m rather than 1 m.

2.4 Measurement #4: Test in 2.4 GHz band (Bluetooth Low Energy)

2.4.1 Measurements #4 parameters

Table 10. Measurements #4: test conditions

Name	BlueNRG-2	Units
Sample time	25	seconds

Name	BlueNRG-2	Units
Frequency	2454	MHz
Data rate	1	Mbps
Modulation	2-GFSK	
Frequency deviation	250	kHz
RX bandwidth	1500	kHz
TX power	7	dBm
TX antenna gain	-2.2 dB	dBi
RX antenna gain	-2.2 dB	dBi
TX antenna height	1	m
RX antenna height	1	m
εr	2.5 (sand)	
Board name	STEVAL-IDB008V2	
Author	Sergio Rossi, Raffaele Riva, Salvatore Bonina (STMicroelectronics)	
Date	11 October 2019	
Location	Ocean Beach San Francisco, California, USA	

Figure 21. Measurement #4 location

2.4.2 Measurements #4 results

Figure 22. **Measurement #4: RSSI vs. distance 2.4 GHz**

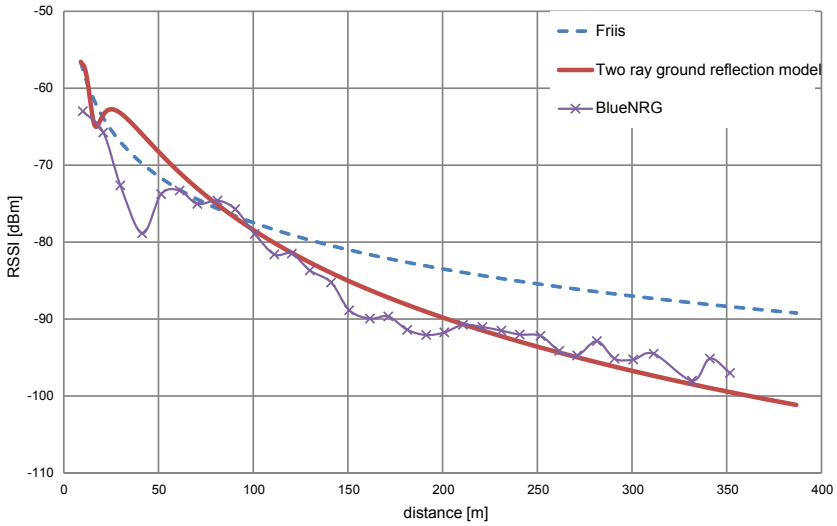

Figure 23. **Measurement #4: packet error rate vs. distance**

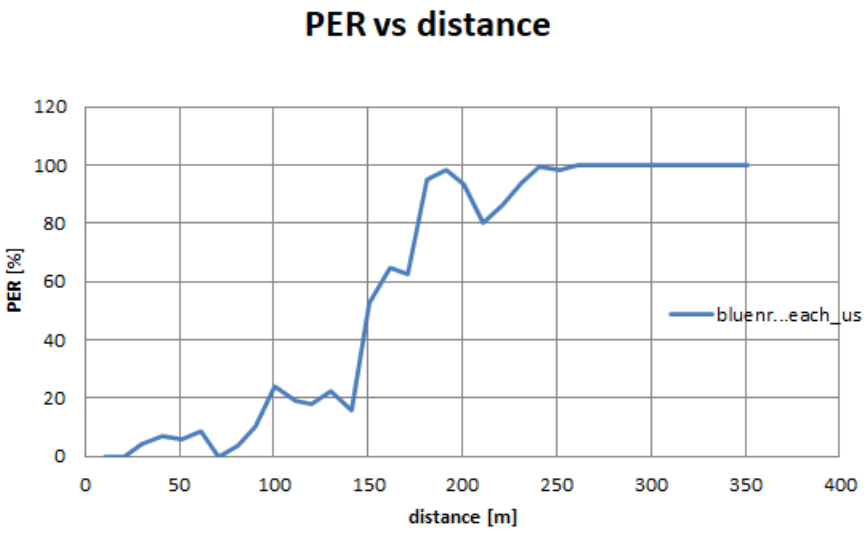

The test results confirm good accuracy between two-ray ground propagation model and results collected on the field also in 2.4 GHz band. Due to technical reasons, the noise floor with the BlueNRG radio cannot be reported.

3 Debugging procedure

This section describes a step-by-step procedure to identify the causes responsible for a poor communication range.

Some tips are provided in order to help to measure the keys parameters which guarantee the link budget necessary to cover the target distance.

We have identified the key parameters which could have an impact on the range of communication; the suggestion is to check them, before starting the range test on the field.

- Tx output power
- Sensitivity of the receiver
- Frequency alignment between receiver and transmitter
- Floor noise measured with 50 Ohm load on SMA antenna port connector
- Antenna gain
- Self-jamming

This procedure consists of two separated kind of measurements: conducted and radiated mode

3.1 Evaluation of the receiver performance in conducted mode

The conducted measurement is done by disconnecting the antenna from the RF port and connecting the PCB directly to instruments such as: spectrum analyzer, signal generator, and power meter via a coaxial cable. The conducted measurements are essential to verify RF performance parameters such as: transmit power level, floor noise, receiver sensitivity and frequency alignment between receiver and transmitter.

This section also describes a simple debugging procedure that can be performed by anyone who is not equipped with professional equipment; in this case to evaluate the performance in terms of radio communication distance, we suggest using our evaluation kit as refence and the STSW-S2LP-DK GUI.

3.1.1 Output power

To check the output power is in line with the expectation, it is needed to measure the conducted output power at the SMA connector.

The preferred way to measure the conducted output power is by a spectrum analyzer, connecting the antenna port of the DUT board to the spectrum analyzer by a coax cable and measuring the peak output power with the transmitter in continuous unmodulated tone.

If the spectrum analyzer is not available, an alternative solution is to replace it with an S2-LP evaluation kit; in this case the DUT board must be connected to the evaluation board by semi-rigid coax cable at the SMA connector.

In order to avoid the saturation of the receiver, we suggest attenuating the RF power by a 20 dB RF attenuator block between the transmitter SMA connector and the receiver SMA connector.

With this setting, using the running RSSI tab of the GUI, evaluating the output power of the DUT transmitter is possible. If the output power is lower than the expected value, the root causes can be the layout, schematic, mismatches and radio settings not in line with the reference design.

3.1.2 Practical method to evaluate receiver performances

The sensitivity of the receiver is another fundamental parameter, which must be as close as possible to the value specified in the datasheet. The suggestion is to measure the sensitivity using the packet error rate as indicator of the quality of the radio link. The best way to measure the sensitivity is by a signal generator, but if it is not available, an evaluation kit, configured as transmitter, can be used. DUT and evaluation kit must be connected by semi-rigid coax cable and an attenuator must be used to reduce the power of the transmitted packet down to when the receiver starts to not receive all the packets.

Using the GUI and the transmission test tab, the packet test both on RX and TX nodes can be configured.

This method is not accurate if the real value of the sensitivity needs to be measured and compared with the value reported in the datasheet.

If a second evaluation board is available, the sensitivity of the evaluation kit can be measured in the same way to have a reference that can be used instead of the sensitivity reported in the datasheet. If conducted sensitivity is poor, the possible root cause could be related to PCB layout, RX network mismatches, radio settings not in line with the reference design and a PCB generated noise.

3.1.3 Self-jamming and noise floor

During the design of a PCB, noisy IC components, which can generate and inject noise inside the receiver band, must be identified. This issue is known as self-jamming.

A good isolation of the receiver from noisy components is fundamental so to avoid a poor receiver performance.

To have an indication of the isolation between the receiver from the noisy part of the application board, the noise floor is a useful parameter.

In order to investigate a possible self-jamming phenomenon, the suggestion is to measure RSSI level with a 50 Ohm load connected on the SMA connector and compare it with the theoretical value of floor noise given by Eq. (36).

This comparison gives a good indication of the impact of the whole circuitry on the noise floor level and then on the sensitivity.

The graph below shows the curve of the RSSI levels measured with the STEVAL-FKI433V2 with 50 Ohm load and the theoretical curve of the noise floor (NF=8 and temperature 25 °C) vs. the bandwidth of the channel filter. In this figure, the impact of the circuitry of our evaluation board is 2 dB and it is constant at the channel filter bandwidth variation.

Figure 24. Noise floor vs. channel filter bandwidth

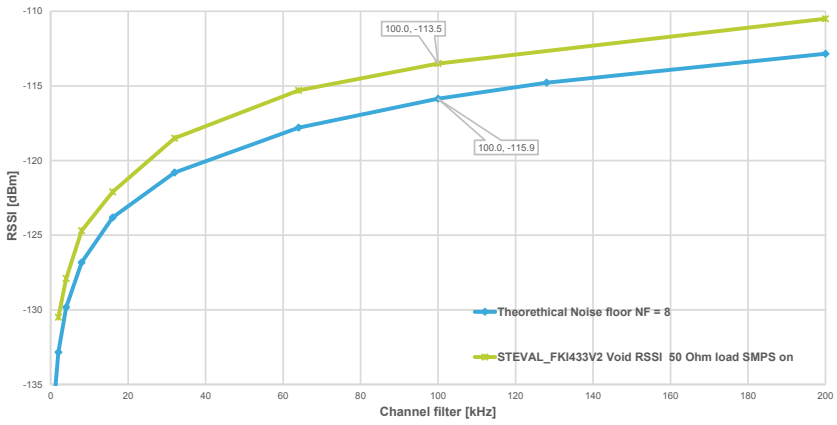

3.1.4 Frequency alignment between receiver and transmitter

The choice of the receiver bandwidth filter is important to get good sensitivity performance.

The RX filter bandwidth must be higher than the occupied bandwidth of the transmitted signal (OBW) plus the maximum frequency error due to crystal inaccuracies.

For narrow band application, the frequency offset between transmitter and receiver must be evaluated due to the inaccuracy of the crystal, which must be considered when the RX filter is chosen.

Moreover, if an XO is used for narrowband applications, then the crystal must be calibrated at manufacturing and a temperature compensation loop may be necessary to compensate the frequency drift due to the temperature.

So, at very low data rate applications, a reference with high frequency stability such as a TCXO must be considered.

The misalignment due to the inaccuracy of the crystal can be the cause of a poor sensitivity and a simple test to verify if the poor sensitivity is due to a frequency offset between RX and TX, is to increase the Rx filter bandwidth on the receiver, for instance increasing by 20%. If the sensitivity improves, then the problem is due to inaccuracy of crystals.

Some of ST's evaluation kits mount a crystal of 50 MHz with ±10 ppm at 25 °C and ±12 ppm frequency drift versus temperature (at -30 to +85 °C); so, the total accuracy of the crystal including initial tolerance and temperature drift is ±22 ppm.

As our kits are frequency-calibrated at manufacturing, the frequency drift only has to be considered due to the temperature. The worst-case scenario occurs if the crystal TX and RX errors have opposite signs.

If the center frequency of the transmitter is 868 MHz, and a crystal error of + 12 ppm is assumed, the maximum frequency deviation is given by 868x 12 = 10.416 kHz.

On the receiver side, if we consider a crystal error of -12 ppm, even if the LO is programmed at 867.7 MHz, we can approximate with the same the error of the carrier frequency; so the frequency deviation is -10.416 kHz. The total maximum frequency misalignment is 20.832kHz.

Figure 25. Channel filter bandwidth vs. XTAL inaccuracy

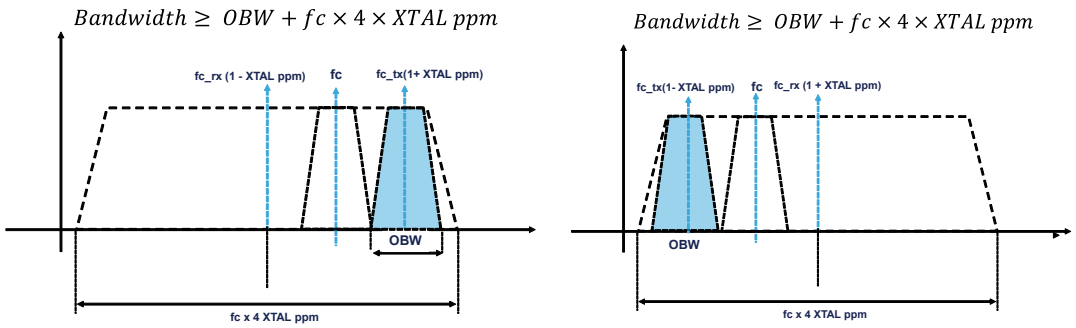

The figure shows the required minimum bandwidth of the channel filter, in the worst case, when the crystal error between transmitter and receiver is maximum and with opposite sign.

3.2 Over the air test using evaluation kit as reference

This section describes a simple procedure to evaluate the performance of the board in terms of radio propagation in open field. The board under test is evaluated using our evaluation kit as references.

The first suggestion is to find a flat area, without obstacles so as to have a line of sight propagation condition.

An area of 200 meters is suggested for the STEVAL-IDB00xVx and 2000-3000 meters for the STEVAL-FKIxxx.

Two evaluation kits are used as references, one for the RX node and one for the TX node, both connected to a different PC and configured by the GUI software.

RX and TX nodes should be placed at a fixed height from the ground, for instance 1.5 meters, with the antenna in a vertical position with respect to the ground.

The procedure can be divided into three parts:

- Environment noise floor
- Path loss estimation at a short distance
- Packet error rate

Figure 26. **Test bench for radio communication test**

3.2.1 Environment noise floor

S2-LP RX node

A good starting point is the measurement of the environment noise floor with TX node off; this measurement can be carried out using the running RSSI function available on the GUI in the running RSSI tab. This simple test estimates the noise floor level measured by the DUT and gives an indication on the noise generated by the circuitry and captured by the antenna. Moreover, the measured noise floor has a direct impact on the link budget. In order to have a realistic value for the budget link, the suggestion is to use the measured noise floor to estimate the minimum power level of the received signal, which guarantees a good reception of the packets.

Figure 27. **Running RSSI tab**

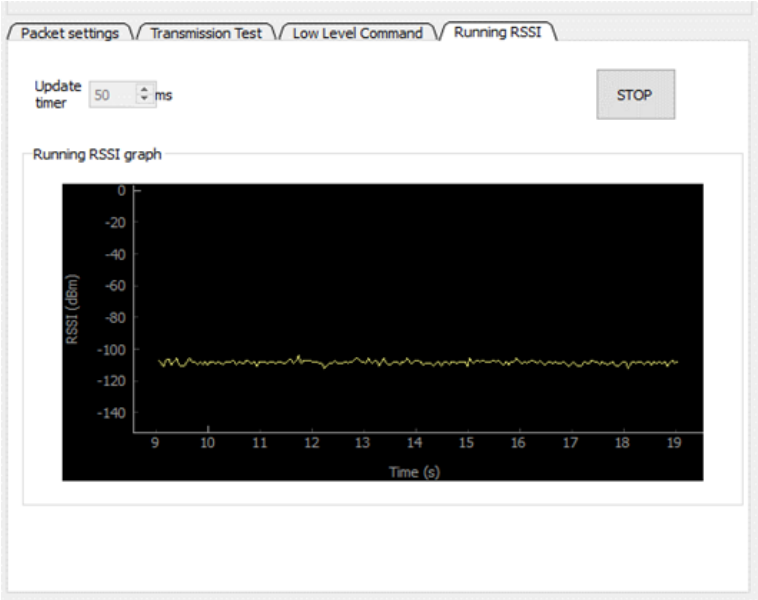

DUT RX node

Repeat the same measurement with the board under test and compare the result with the S2-LP reference board.

This simple test allows the noise floor level measured by the DUT to be estimated and gives an indication on the noise generated by the circuitry and captured by the antenna. Moreover, the measured noise floor has a direct impact on the budget link. In order to have a realistic value for the budget link, the suggestion is to use the measured noise floor instead of the sensitivity reported in the datasheet.

3.2.2 Received power at short distance

Before moving the RX and TX nodes away, a simple test is suggested to be performed, with RX and TX nodes placed at short distance, for instance 50 meters for sub 1-GHz and 10 meters for BLE, with the purpose of comparing the level of power received with noise floor measured in the previous step. An indication of your potential link budget is thus given.

Considering the Friis equation, the path loss exponent in line of sight condition is 2, it means that 6 dB are needed to double the distance.

In our experiments, we observed that the path loss exponent is higher than two and we estimated that at least 10 dB are needed to double the communication distance.

The TX node, placed at 50 meters from the RX node, must be configured to transmit a single tone at the maximum power. The RX node in continuous RX mode must read the RSSI using the running RSSI function.

Now, knowing the difference between the power level of the received signal and floor noise, the communication distance can be estimated considering that 10 dB are necessary to double the distance.

For instance, if the received power at 50 meters is -50 dBm and the floor noise is -110 dBm, considering we start losing packets at -100 dBm (10 dB above the floor noise), the link budget is 50 dB, which means that we can double the distance 5 times and estimate a distance of 1.6 km.

This simple way to estimate the range is valid if LOS condition is guaranteed in the whole path.

The experiment should also be repeated with the evaluation kit to obtain a reference.

3.2.3 Packet error rate estimation

Place RX node at a fixed position connected to a PC with the antenna in a vertical position with respect to the ground.

The RX node must be configured in packet reception mode in order to log all the received packets. Please collect at least 250/500 packets to make a statistical, meaningful calculation.

The second evaluation kit must be configured as transmitter node and we suggest to start the test placing the TX node with antenna in a vertical position with respect to the ground.

In order to use the two-ray model it is important to record also the height from the ground of both nodes.

3.2.4 Estimation using log-distance path loss model for 868 MHz

This section describes how to apply the log-distance path loss to estimate path loss. To validate the method we have used experimental data recorded during a radio range communication test done with ST's STEVAL-FKI868V2 evaluation kit. The environmental parameters and device settings used in this experiment are described in the previous sections.

Table 11. RSSI samples at difference distances

Sample points	distance [m]	rssi average [dBm]
1	50.36	-47.91
2	99.56	-60.09
3	200.11	-66.38
4	299.89	-75.81
5	400.98	-85.12
6	500.73	-85.92
7	600.97	-89.39
8	700.45	-91.27
9	799.68	-94.63
10	901.2	-96.18
11	1002.69	-94.82
12	1098.91	-96.14
13	1200.38	-98.43
14	1302.51	-100.38
15	1405.42	-101.34
16	1501.54	-101.23
17	1600.22	-103.67
18	1703.47	-105.68
19	1806.61	-106.97
20	1901.7	-105.55
21	2002.36	-107.15
22	2202.07	-107.86
23	2400.98	-111.72
24	2498.12	-108.85
25	2704.19	-109.34

In Table 11. RSSI samples at difference distances all the RSSI samples are listed at different distances recorded during the measurement #2 at 868 MHz. Five sample points have been selected to calculate the path loss exponent which characterizes our test environment.

Table 12. Samples used to determinate the path loss exponent

	Distance [m]	RSSI average [dBm]
$P_r(d_0)$	99.56	-60.09
$P_r(d_1)$	200.11	-66.38
$P_r(d_2)$	299.89	-75.81
$P_r(d_3)$	400.98	-85.12
$P_r(d_4)$	799.68	-94.63

Let $P_r(d_i)$ the measured received power and $P(d_i)$ the estimated power at a distance d_i

$$\widehat{P_r}(d_0) = P_r(d_0) - 10n\log\left(\frac{d_0}{d_0}\right) = P_r(d_0) = -60 \quad (53)$$

$$\widehat{P_r}(d_1) = P_r(d_0) - 10n\log\left(\frac{d_1}{d_0}\right) = P_r(d_0) - 10n\log\left(\frac{200}{100}\right) = -60 - 3n \quad (54)$$

$$\widehat{P_r}(d_2) = P_r(d_0) - 10n\log\left(\frac{d_1}{d_0}\right) = P_r(d_0) - 10n\log\left(\frac{300}{100}\right) = -60 - 4.7n \quad (55)$$

$$\widehat{P_r}(d_3) = P_r(d_0) - 10n\log\left(\frac{d_2}{d_0}\right) = P_r(d_0) - 10n\log\left(\frac{400}{100}\right) = -60 - 6n \quad (56)$$

$$\widehat{P_r}(d_4) = P_r(d_0) - 10n\log\left(\frac{d_3}{d_0}\right) = P_r(d_0) - 10n\log\left(\frac{800}{100}\right) = -60 - 9n \quad (57)$$

The sum of the squared error between the measured and the estimated values is given:

$$\text{MMSE} = \sum_i \left(P_r(d_i) - \widehat{P_r}(d_i)\right)^2 \quad (58)$$

$$\text{MMSE} = [-66.38 - (-60 - 3n)]^2 + [-75.81 - (-60 - 4.7n)]^2 + [-85.12 - (-60 - 6n)]^2 + [-94.63 - (-60 - 9n)]^2 = 148.09n^2 - 1111.674n + 2120.918 \quad (59)$$

$$\frac{d}{dn}(\text{MMSE}) = 0\ ;\ n = 3.75 \quad (60)$$

$$\overline{P_R}(dB) = \overline{P_R}(d_0) + 3.75 \times 10\log\left(\frac{d}{d_0}\right) = -60 + 3.75 \times 10\log\left(\frac{d}{100}\right) \quad (61)$$

The image below shows the behavior of three different kinds of path loss models: Friis, two-ray model and log-distance path loss model. In the same graph, the data measured from received power during the communication range experiment performed with our STEVAL-FKI868V2. The image highlights the difference between the three different path loss models.

The coefficient n of the log-distance path loss model has been calculated using the first four measurements and shows a good estimation of the real path loss behavior.

Figure 28. Propagation loss models comparison at 868 MHz

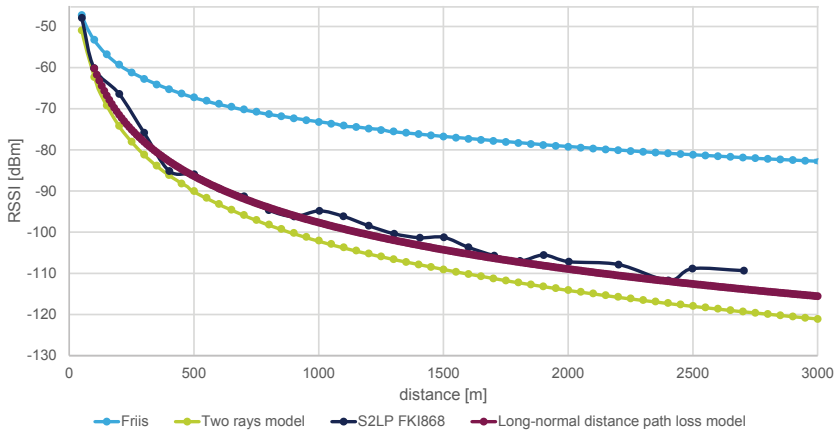

3.2.5 Estimation using log-distance path loss model for 433 MHz

This section describes how to apply the log-distance path loss to estimate path loss. To validate the method we used experimental data recorded during a radio range communication test with the ST STEVAL-FKI433V2 evaluation kit. The environmental parameters and device settings used in this experiment are described in Section 3.2.4 Estimation using log-distance path loss model for 868 MHz.

Table 13. RSSI samples at different distances

Distance [m]	RSSI average [dBm]
102.17	-69.14
203.23	-77.24
301.98	-72.96
501.77	-87.43
605.21	-92
703.38	-99.31
804.32	-96.44
901.6	-107.31
954.08	-107.14

$$n = \frac{\Sigma_i \left[(P_{d0} - P_{di}) \times 10\log\left(\frac{d_i}{d_0}\right) \right]}{\Sigma_i \left[10 \times \log\left(\frac{d_i}{d_0}\right) \right]^2} \quad (62)$$

The path loss coefficient n calculated is 3.32 and shows a good estimation of the real path loss behavior.

Figure 29. Propagation loss models comparison at 433 MHz

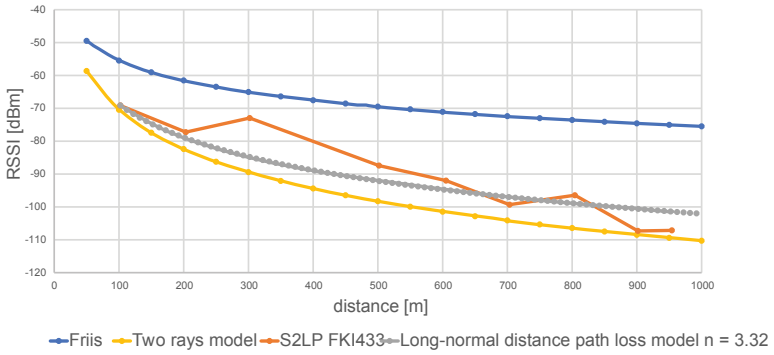

3.3 Antenna matching

If the conducted sensitivity and conducted output power are as expected, but the distance of communication is lower than that achievable by evaluation kits then very likely the responsibility of this poor performance is the antenna efficiency.

To obtain the maximum transfer of RF energy from the transmission line into the antenna, the antenna impedance should be as close as possible to the characteristic impedance of the transmission line, at the operating frequency; in this case antenna and transmission line are considered matched.

If antenna impedance and transmission line are mismatched not all the energy is transferred from the transmission line into the antenna. The energy not transferred into the antenna is not irradiated and it is reflected back on the transmission line.

A parameter measuring the mismatch between antenna and transceiver is the voltage standing wave ratio (VSWR).

VSWR is the ratio between the maximum and the minimum amplitude of a standing wave measured along a transmission line, which connects the transceiver to the antenna.

VSWR is a function of the reflection coefficient, which describes the power reflected from the antenna. If the reflection coefficient is given by S11, then the VSWR is defined by the following formula:

$$VSWR = \frac{1 + |S_{11}|}{1 - |S_{11}|} \quad (63)$$

The lower the VSWR, the better the radio performs; good performance can be achieved by values of VSWR lower than 2 dB. For instance, with an VSWR of 2.1 the S11 is 9 dB.

An antenna needs to resonate at the operating frequency to maximize its radiation. The resonance frequency is where the impedance of the inductance XL equals the impedance of the capacitance XC. So, at the resonance frequency the antenna appears purely resistive.

The resistance is a combination of loss resistance and radiation resistance. For an optimized system, the impedance seen in the antenna should match the characteristic impedance (system impedance), which is normally 50 Ohm.

A single-ended monopole antenna requires an associated ground plane to form a dipole antenna; so, the ground plane can be considered as the ‘second half’ of the antenna. The shape and size of the ground plane affects the center frequency and the bandwidth. For this reason, the reflection coefficient must be measured with the antenna placed on the PCB. The effects of the housing and of the proximity of any circuit elements have to be considered; therefore, the matching network should be defined in this condition.

3.4 Self-jamming. Debug of the receiver in radiated mode

The purpose of this section is to provide a debug procedure to discover the possible root causes of a poor range of communication even if all tests in conducted mode have been fulfilled successfully.

The optimization of the conducted sensitivity and the conducted output power is a time-consuming activity, but it does not guarantee to reach the expected distance of communication.

The radiated test allows the RF performance of the whole system as in current use, to be estimated, where a real interaction among the antenna, PCB and final enclosure is present.

Thanks to the radiated test it is possible, for instance, to discover self-jamming phenomena like emissions coming from some noisy part of the circuitry itself that may lead to the creation of spurs that exceed the allowed interference level.

In this section we suggest a test setup to investigate a possible self-jamming without the use of an anechoic chamber.

The board under test is placed inside an RF shielded box in order to reduce the environment noise floor and to be able to capture the noise coming from the board itself. The RF box is equipped with an SMA RF connector which allows either a spectrum or a signal generator to be connected. Figure 30. Test bench for test in radiated mode shows a possible test bench.

The spectrum analyzer is used to measure the noise captured by the antenna mounted on the board under test inside the RF box; in this case the STEVAL-FKI868V2 evaluation kit is the device under test.

In order to measure the noise captured by the antenna mounted on the PCB, we disconnect the RX and TX paths from the SMA connector removing the C16 and C21 capacitors (see Figure 32) and we solder an RF cable on the back side of the SMA connector.

Figure 30. **Test bench for test in radiated mode**

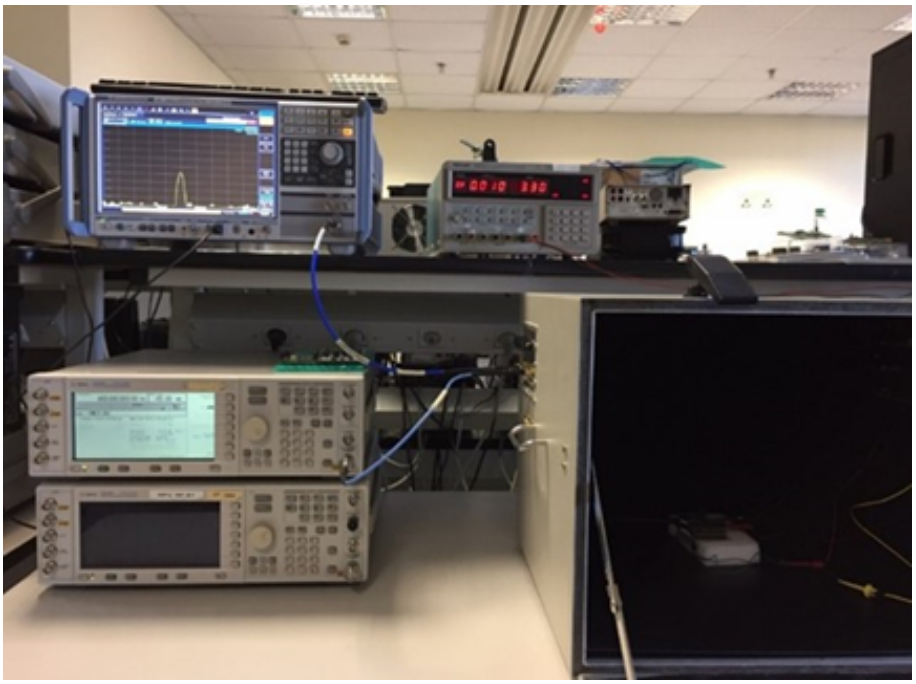

Figure 31. **STEVAL-FKI433 MHz RX and TX paths**

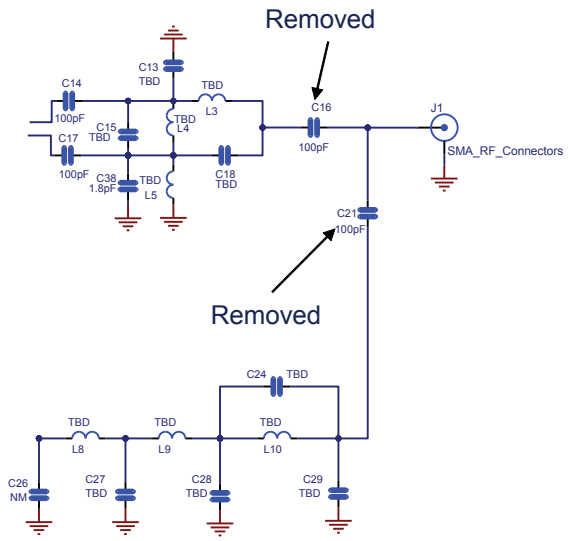

So now we have a test bench to measure the floor noise captured by the antenna used by the application and placed on the board in its final position. The first measurement must determinate the zero level of the noise floor when the DUT is not supplied.

The second step is to supply the DUT and check the noise floor to compare it with the level measured with DUT not supplied.

The test can be performed configuring the board in different ways in order to check if some blocks of the board have a non negligible impact on the noise, for instance, SPI communication, DC-DC converters.

3.5 STEVAL kit radiation patterns

A fundamental step for the validation of evaluation kits is the measurement of critical antenna parameters like gain, radiation efficiency and radiation patterns. The radiation characterization of the whole system, PCB plus antenna, has also been important to validate the range estimation model.

Radiation pattern can be defined as the graphical representation of the radiative properties of an antenna.

The standard coordinate system used to represent the radiation properties is a spherical coordinate system.

3D EIRP patterns in far field region is chosen to determine the radiation pattern of an antenna as function of directional coordinates. The total radiated power (TRP) of the transmitter, based on the spherically integrated EIRPs in any 3D pattern has been calculated.

Thanks to 3D spherical patterns it is possible to discover unexpected disturbances in patterns that can come from feed line, enclosure or PCB edge interaction.

The radiation pattern of our kit is measured programming the radio as transmitter in CW mode at the maximum output power.

The evaluation kit under test is rotated by a turn table from 0° to 180° and the turn arm is rotated 360° so a 3D radiation diagram can illustrate the spacial distributions.

3.5.1 STEVAL-FKI868V2

The part number of the antenna used for the communication range test is ANT-900MS.

Figure 32. STEVAL-FKI868V2 vertical polarization

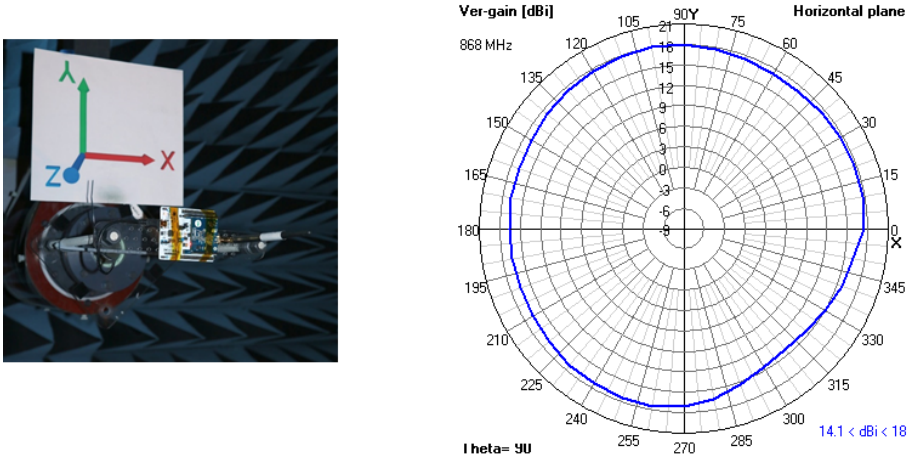

Figure 33. STEVAL-FKI8682 3D radiation patter

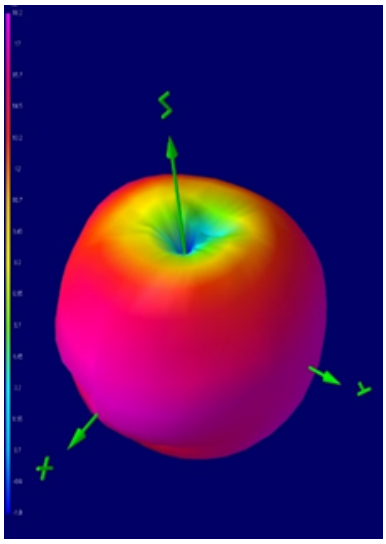

The difference between the power measured in conducted mode (15.83 dBm) and the total radiated power (14.8 dBm) gives the efficiency of the antenna; in this case 1 dB is lost only.

The power measured on +X direction (theta = 90°, phi = 0°) is 17.4 dBm. The gain of the antenna is given by 17.4 - 14.8 = 2.6 dB 17.4 - 15.83 = 1.57 dBm.

The 3D representation of the radiation pattern shows the distribution in the space of the gain expressed in dBi. In this figure the typical “doughnut” pattern distortion of a dipole antenna in the -Z axis is well recognizable, due to feed line radiation (the feed line extends from this dipole in the +Z axis.

For horizontal polarization.

3.5.2 STEVAL-FKI433V2

The part number of the antenna used for communication range test is ANT-418-CW-HWR.

Figure 34. STEVAL-FKI433V2 vertical polarization

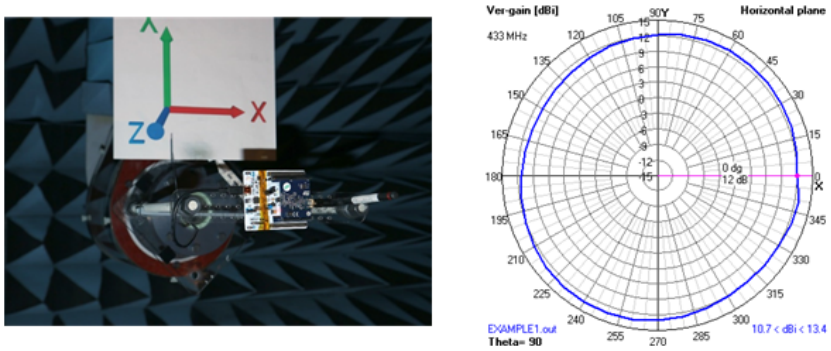

Figure 35. STEVAL-FKI433V2 3D radiation pattern

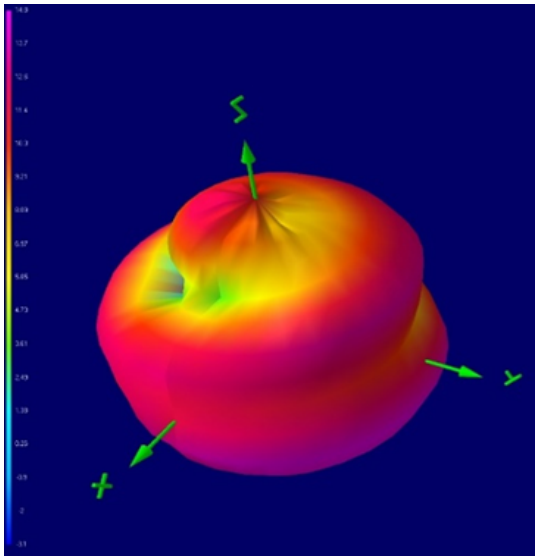

The efficiency given by conducted power menus total radiated power is: 14.31 dBm – 11.4 dBm = -2.91 dBm. This result demonstrates the 433 MHz antenna is less efficient than the 868 MHz case. The power measured on +X direction (theta = 90°, phi = 0°) is 12 dBm. Considering the transmitter power measured in conducted mode (14.31 dBm) the gain of the antenna in its maximum power direction is given by:

– (14.31 dBm - 12 dBm) = - 2.31 dB

3.5.3 STEVAL-IDB008V1

Figure 36. **STEVAL-IDB008V1 vertical polarization**

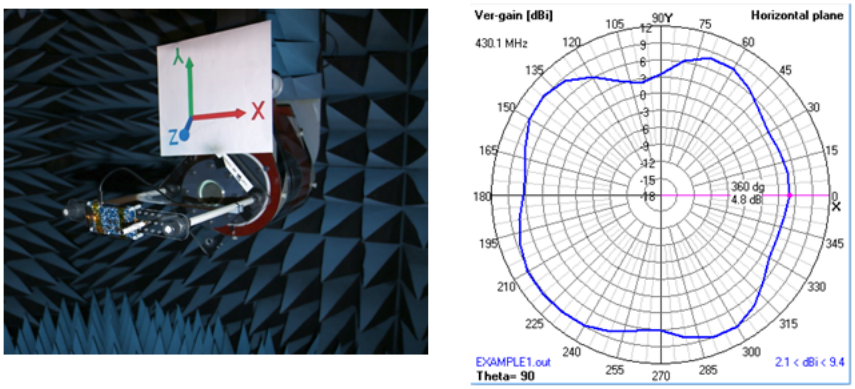

Figure 37. **STEVAL-IDB008V1 3D radiation pattern**

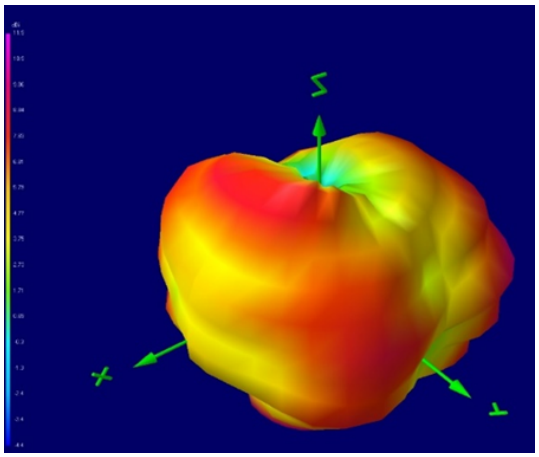

The power measured on +X direction (theta = 90°, phi = 0°) is 4.8 dBm. The gain of the antenna is -2.2 dB.

4 List of acronyms and abbreviations

Acronym / abbreviation	Description
ACP	Adjacent channel power
BER	Bit error rate
FSK	Frequency-shift keying
GFSK	Gaussian frequency-shift keying
PER	Packet error rate
ERP	Effective radiated power
EIRP	Effective isotropic radiated power
FEC	Forward error correction
OFSK	Orthogonal frequency-shift keying
RBW	Resolution bandwidth
VBW	Video bandwidth
VSWR	Voltage standing wave ratio

5 Bibliography

[1] T. S. Rappaport, Wireless Communications: Principles and Practice (2nd Edition), Prentice Hall, 2015.

[2] F. Dressler and C. Sommer, "Using the Right Two-Ray Model? A Measurement-based Evaluation of PHY Models in VANETs," in *17th ACM International Conference on Mobile Computing and Networking (MobiCom 2011)*, Las Vegas, NV, 2011.

[3] A. F. ANT-418-CW-HWR, "https://www.linxtechnologies.com/wp/wp-content/uploads/ant-418-cw-hwr.pdf," [Online].

[4] L. p. r. ANT-900MS, "http://www.lprs.co.uk/assets/files/downloads/ant-900mrms-antenna-datasheet-v1.3.pdf," [Online].

Revision history

Table 14. **Document revision history**

Date	Version	Changes
03-Nov-2020	1	Initial release.
07-Jul-2022	2	Updated Figure 19. Measurement #3 RSSI vs. distance, Section 3.1.2 Practical method to evaluate receiver performances and Section 3.1.3 Self-jamming and noise floor.

Contents

1 **Radio signal propagation introduction 2**
1.1 Free space propagation model 2
1.2 Multi-path propagation 3
1.3 Ground reflection model 3
1.4 Two-ray ground propagation model 6
1.5 Log-distance path loss model 8
1.6 Antenna parameters 8
1.7 Noise floor 10
1.8 Sensitivity 11
1.9 Summary 12
2 **Experimental results 15**
2.1 Measurement #1: logarithmic trend of RSSI 16
2.1.1 Measurement #1 parameters 16
2.1.2 Measurement #1 results 17
2.2 Measurement #2: comparison between 433 MHz and 868 MHz band 18
2.2.1 Measurements #2 parameters 18
2.2.2 Measurement #2 results 19
2.2.3 Measurement #2 analysis 21
2.3 Measurement #3: Test in 433 MHz band 21
2.3.1 Measurements #3 parameters 21
2.3.2 Measurements #3 results 23
2.4 Measurement #4: Test in 2.4 GHz band (Bluetooth Low Energy) 23
2.4.1 Measurements #4 parameters 23
2.4.2 Measurements #4 results 25
3 **Debugging procedure 26**
3.1 Evaluation of the receiver performance in conducted mode 26
3.1.1 Output power 26
3.1.2 Practical method to evaluate receiver performances 26
3.1.3 Self-jamming and noise floor 27
3.1.4 Frequency alignment between receiver and transmitter 27

3.2 Over the air test using evaluation kit as reference 28
3.2.1 Environment noise floor 29
3.2.2 Received power at short distance 30
3.2.3 Packet error rate estimation 30
3.2.4 Estimation using log-distance path loss model for 868 MHz 31
3.2.5 Estimation using log-distance path loss model for 433 MHz 33
3.3 Antenna matching 33
3.4 Self-jamming. Debug of the receiver in radiated mode. 34
3.5 STEVAL kit radiation patterns 36
3.5.1 STEVAL-FKI868V2 36
3.5.2 STEVAL-FKI433V2 37
3.5.3 STEVAL-IDB008V1 38
4 List of acronyms and abbreviations 39
5 Bibliography. 40
Revision history 41

List of tables

Table 1. Path loss exponent for different environments . . . 8
Table 2. Radio communication range key parameters . . . 13
Table 3. Radio communication range model parameters . . . 15
Table 4. Measurement #1 test conditions . . . 16
Table 5. Input data used in the mathematical model . . . 17
Table 6. Measurement #2 test conditions . . . 18
Table 7. Noise floor comparison 433 MHz vs. 868 MHz . . . 19
Table 8. Comparison between 433 MHz and 868 MHz . . . 21
Table 9. Measurements #3: test conditions . . . 21
Table 10. Measurements #4: test conditions . . . 23
Table 11. RSSI samples at difference distances . . . 31
Table 12. Samples used to determinate the path loss exponent . . . 32
Table 13. RSSI samples at different distances . . . 33
Table 14. Document revision history . . . 41

List of figures

Figure 1. Reflection model . . . 4
Figure 2. Reflection coefficient vs. incident angle for sand (ε_r=2.5) . . . 4
Figure 3. Module of reflection coefficient vs. incident angle for sand (ε_r=2.5) . . . 5
Figure 4. Reflection coefficient vs. incident angle for soil (ε_r=18) . . . 5
Figure 5. Module of reflection coefficient vs. incident angle for soil (ε_r=18) . . . 6
Figure 6. 2-ray ground reflection diagram . . . 6
Figure 7. Antenna radiation pattern example . . . 9
Figure 8. Power flux density at a distance d from a point source . . . 10
Figure 9. BER vs. Eb/N0 for FSK and ASK modulation . . . 12
Figure 10. Radio communication range key parameters . . . 13
Figure 11. Measurement #1 location . . . 16
Figure 12. RSSI vs. distance at 433 MHz . . . 17
Figure 13. Measurement #2 location (868 MHz) . . . 18
Figure 14. Measurement #2 location (433 MHz) . . . 19
Figure 15. RSSI vs. distance (868 MHz) . . . 20
Figure 16. RSSI vs. distance (433 MHz) . . . 20
Figure 17. Packet error rate vs. distance (433 MHz) . . . 21
Figure 18. Measurement #3 location . . . 22
Figure 19. Measurement #3 RSSI vs. distance . . . 23
Figure 20. Measurement #3: packet error rate vs. distance . . . 23
Figure 21. Measurement #4 location . . . 24
Figure 22. Measurement #4: RSSI vs. distance 2.4 GHz . . . 25
Figure 23. Measurement #4: packet error rate vs. distance . . . 25
Figure 24. Noise floor vs. channel filter bandwidth . . . 27
Figure 25. Channel filter bandwidth vs. XTAL inaccuracy . . . 28
Figure 26. Test bench for radio communication test . . . 29
Figure 27. Running RSSI tab . . . 30
Figure 28. Propagation loss models comparison at 868 MHz . . . 32
Figure 29. Propagation loss models comparison at 433 MHz . . . 33
Figure 30. Test bench for test in radiated mode . . . 35
Figure 31. STEVAL-FKI433 MHz RX and TX paths . . . 35
Figure 32. STEVAL-FKI868V2 vertical polarization . . . 36
Figure 33. STEVAL-FKI8682 3D radiation patter . . . 36
Figure 34. STEVAL-FKI433V2 vertical polarization . . . 37
Figure 35. STEVAL-FKI433V2 3D radiation pattern . . . 37
Figure 36. STEVAL-IDB008V1 vertical polarization . . . 38
Figure 37. STEVAL-IDB008V1 3D radiation pattern . . . 38